US010261106B2

(12) **United States Patent**
Aksyuk et al.

(10) **Patent No.: US 10,261,106 B2**
(45) **Date of Patent: Apr. 16, 2019**

(54) **PHOTONIC PROBE FOR ATOMIC FORCE MICROSCOPY**

(71) Applicant: **The United States of America, as represented by the Secretary of Commerce**, Washington, DC (US)

(72) Inventors: **Vladimir Aksyuk**, Gaithersburg, MD (US); **Marcelo Davanco**, Rockville, MD (US)

(73) Assignee: **THE UNITED STATES OF AMERICA, AS REPRESENTED BY THE SECRETARY OF COMMERCE**, Washington, DC (US)

(*) Notice: Subject to any disclaimer, the term of this patent is extended or adjusted under 35 U.S.C. 154(b) by 0 days.

(21) Appl. No.: **15/799,337**

(22) Filed: **Oct. 31, 2017**

(65) **Prior Publication Data**

US 2018/0172728 A1 Jun. 21, 2018

Related U.S. Application Data

(60) Provisional application No. 62/437,107, filed on Dec. 21, 2016.

(51) **Int. Cl.**
G01Q 20/02 (2010.01)
G01Q 60/38 (2010.01)
(Continued)

(52) **U.S. Cl.**
CPC ***G01Q 20/02*** (2013.01); ***G01Q 20/04*** (2013.01); ***G01Q 60/38*** (2013.01); *G02B 6/1225* (2013.01);
(Continued)

(58) **Field of Classification Search**
None
See application file for complete search history.

(56) **References Cited**

U.S. PATENT DOCUMENTS

8,997,258 B2 3/2015 Aksyuk et al.
10,031,158 B1 * 7/2018 Douglas G01Q 20/02
(Continued)

OTHER PUBLICATIONS

Srinivasan et al., "Optomechanical Transduction of an Integrated Silicon Cantilever Probe Using a Microdisk Resonator", NanoLetters (Year: 2010).*
(Continued)

Primary Examiner — Michael J Logie
(74) *Attorney, Agent, or Firm* — Office of Chief Counsel for National Institute of Standards and Technology

(57) **ABSTRACT**

A photonic probe for atomic force microscopy includes: a cantilever including: a tip; a wing in mechanical communication with the tip; an extension interposed between the tip and the wing to synchronously communicate motion of the tip with the wing; an optical resonator disposed proximate to the cantilever and that: receives input light; and produces output light, such that: the cantilever is spaced by a gap distance from the optical resonator, wherein the gap distance varies as the cantilever moves relative to the optical resonator, and the output light differs from the input light in response to movement of the cantilever relative to the optical resonator; an optical waveguide in optical communication with the optical resonator and that: provides the input light to the optical resonator; and receives the output light from the optical resonator.

8 Claims, 18 Drawing Sheets

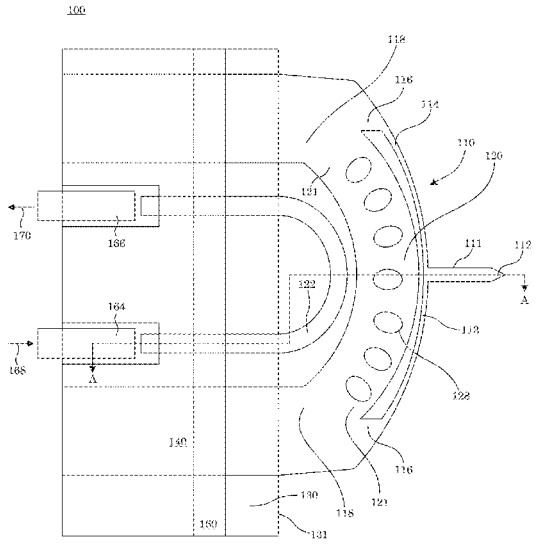

(51) **Int. Cl.**

G01Q 20/04	(2010.01)
G02B 6/122	(2006.01)
G02B 6/293	(2006.01)
H01J 37/317	(2006.01)
H01J 37/302	(2006.01)
G02B 6/12	(2006.01)

(52) **U.S. Cl.**

CPC *G02B 6/29338* (2013.01); *G02B 2006/12138* (2013.01); *H01J 37/3026* (2013.01); *H01J 37/3174* (2013.01)

(56) **References Cited**

U.S. PATENT DOCUMENTS

2014/0047585	A1*	2/2014	Hofrichter	G01Q 20/02 850/56
2014/0338074	A1*	11/2014	Aksyuk	G01Q 20/02 850/6
2018/0113149	A1*	4/2018	Walter	G01Q 20/02
2018/0172728	A1*	6/2018	Aksyuk	G01Q 20/02
2018/0203037	A1*	7/2018	Walter	G01Q 10/045

OTHER PUBLICATIONS

S. An, et al., Optomechanical transducer-based soft and high frequency nanoscale cantilever for atomic force microscopy, Proceedings, Solid State Sensor, Actuator and Microsystems Workshop, 2016, p. 266-269.

J. Zou, et al., Integrated silicon optomechanical transducers and their application in atomic force microscopy, OSA Technical Digest, 2014.

Y. Liu, et al., Wide cantilever stiffness range cavity optomechanical sensors for atomic force microscopy, Optics Express, 2012, p. 18268-18280, vol. 20 No. 16.

K. Srinivasan, et al., Optomechanical transduction of an integrated silicon cantilever probe using a microdisk resonator, Nano Letters, 2011, p. 791-797, vol. 11.

T. Michels, et al., Optical probe for nondestructive wafer-scale characterization of photonic elements, IEEE Photonics Technology Letters, 2017, 643-646, vol. 29 No. 8.

* cited by examiner

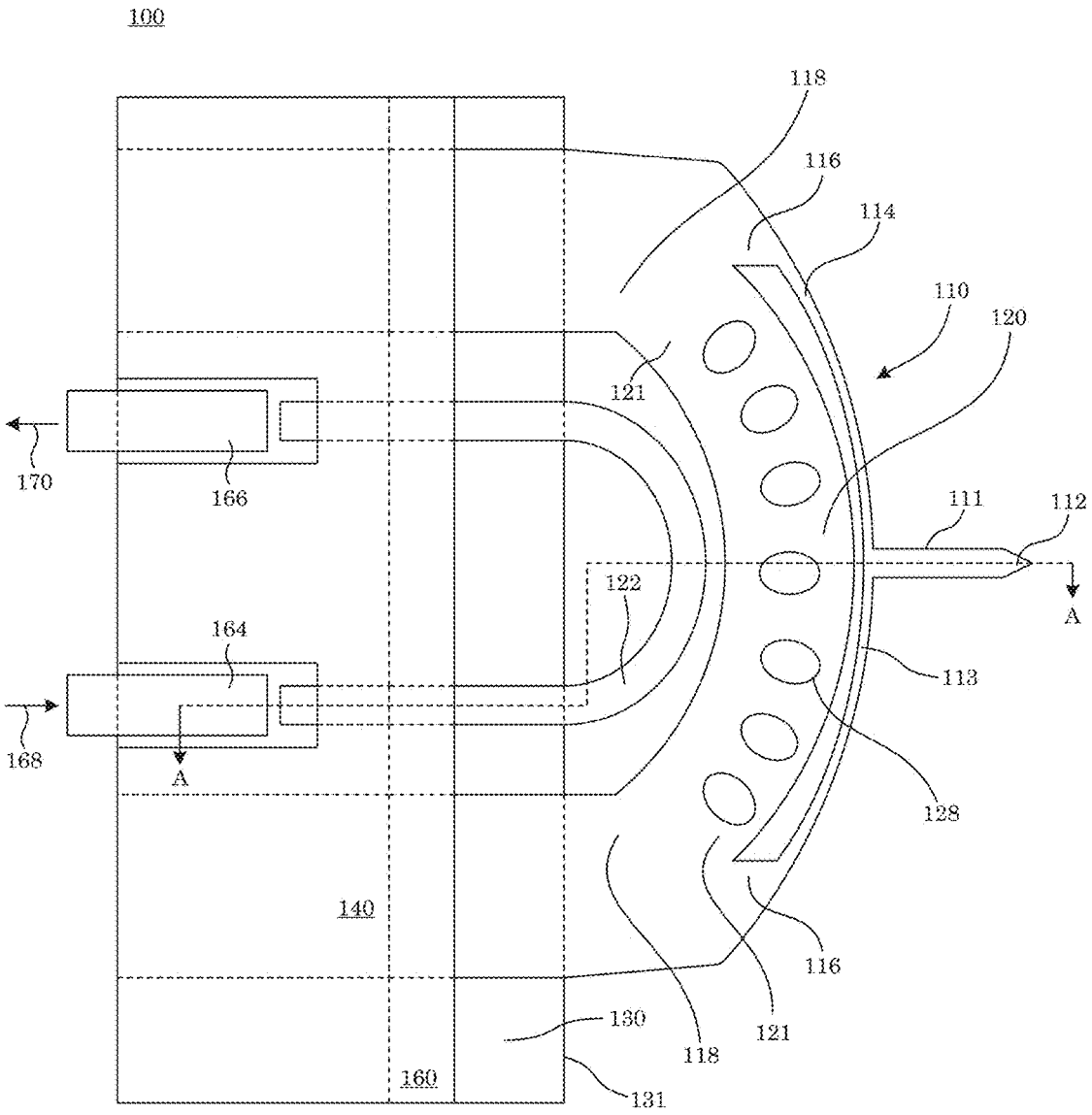
100
118
116
114
110
120
121
170
166
111
112
122
A
164
113
168
A
128
140
116
130
121
118
160
131

Figure 1

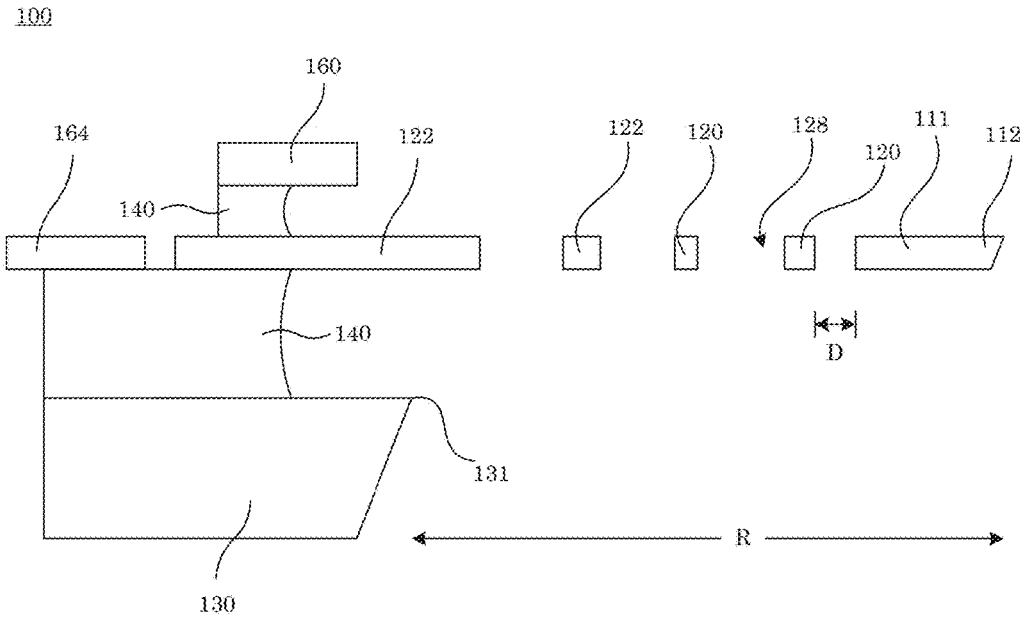

Figure 2

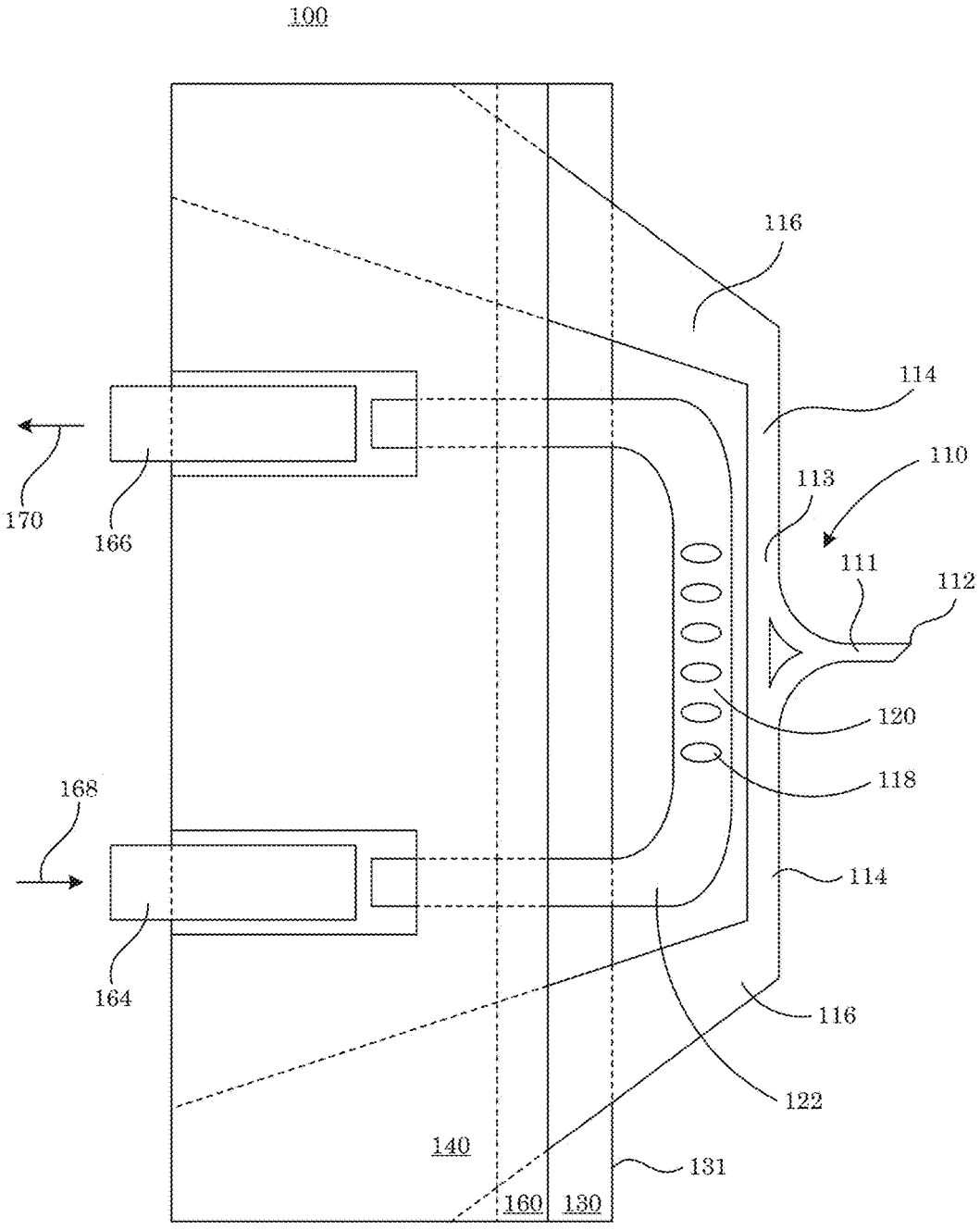
100
116
114
110
113
111
112
120
118
114
116
122
131
140
160
130
170
166
168
164

Figure 3

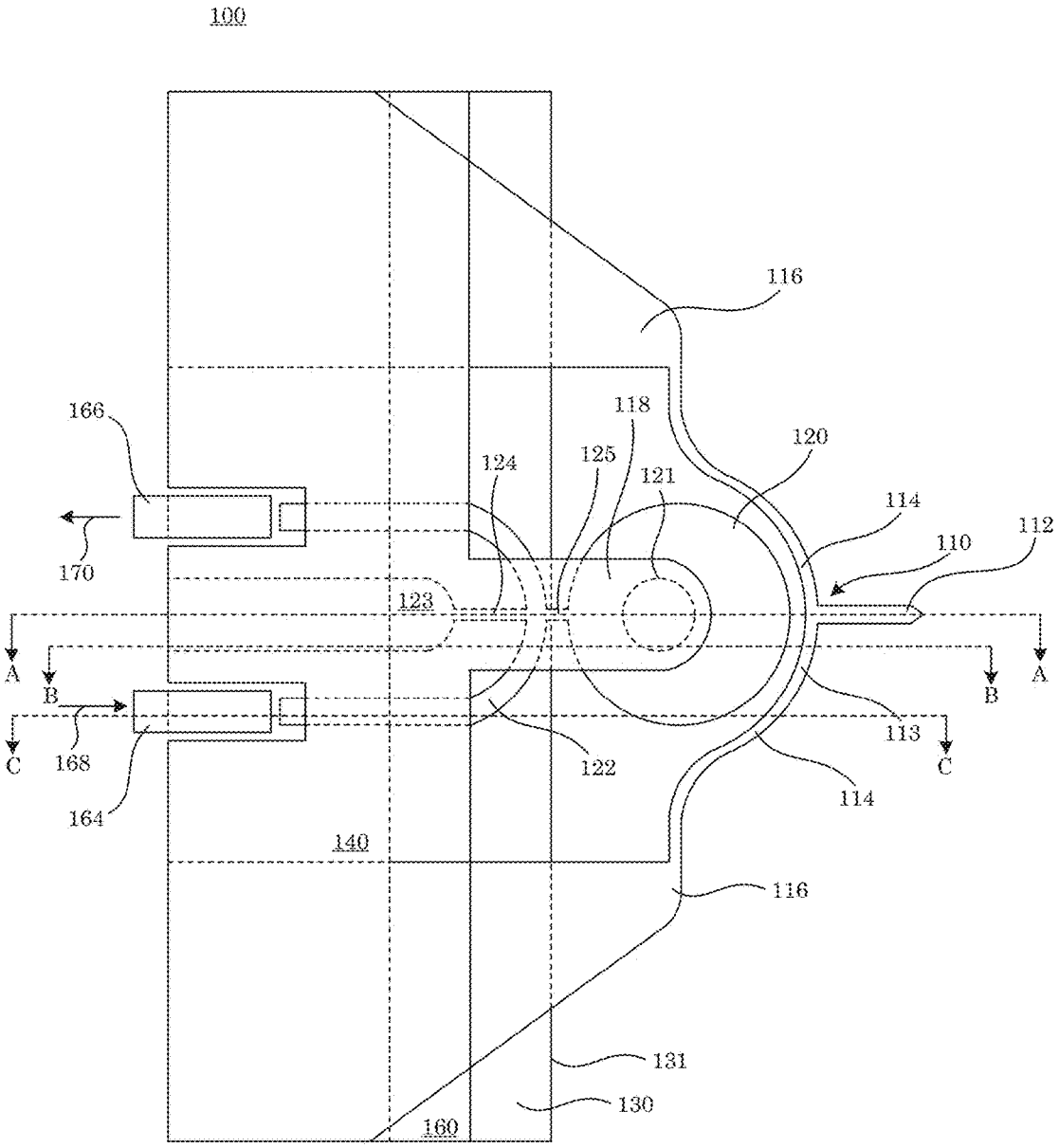
100
116
166
118
120
124
125
121
114
112
110
170
123
A
B
A
B
C
168
122
113
C
164
114
140
116
131
130
160

Figure 4

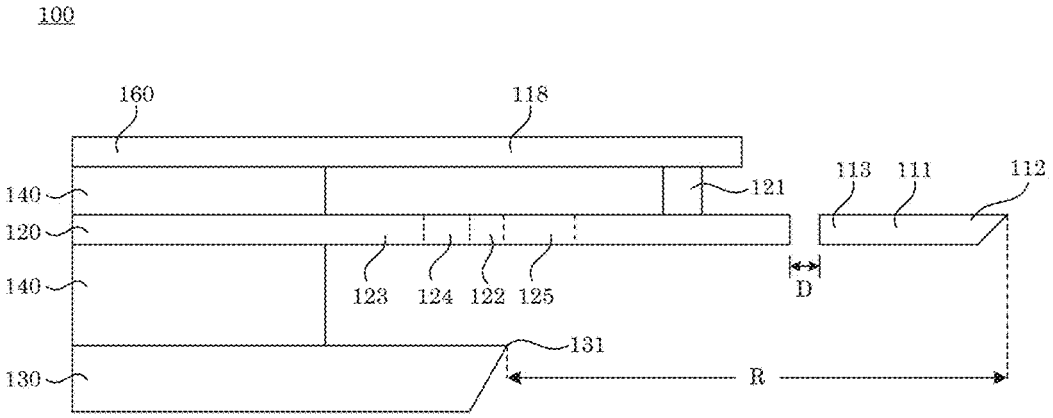
100
160
118
140
120
140
130
121
113
111
112
123
124
122
125
D
131
R

Figure 5

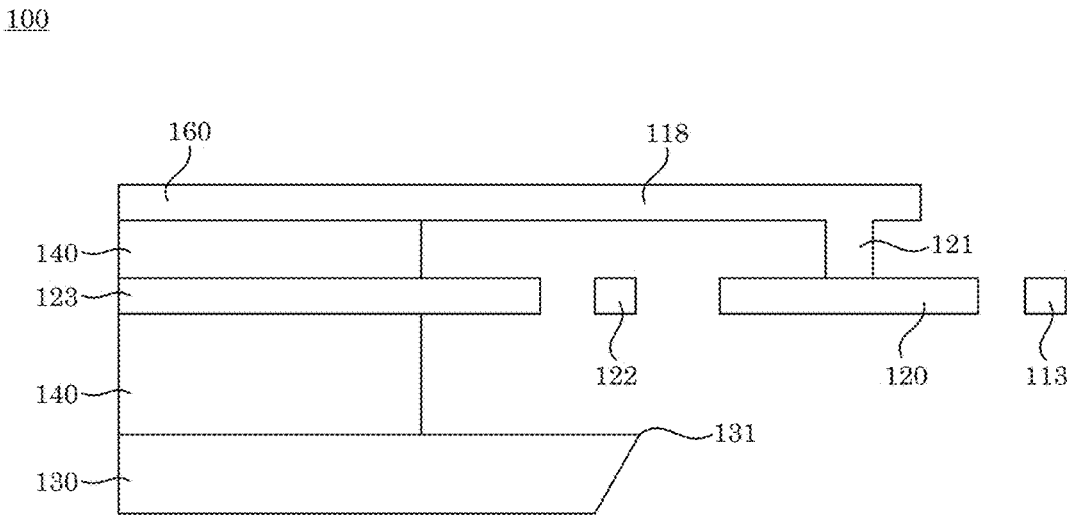

Figure 6

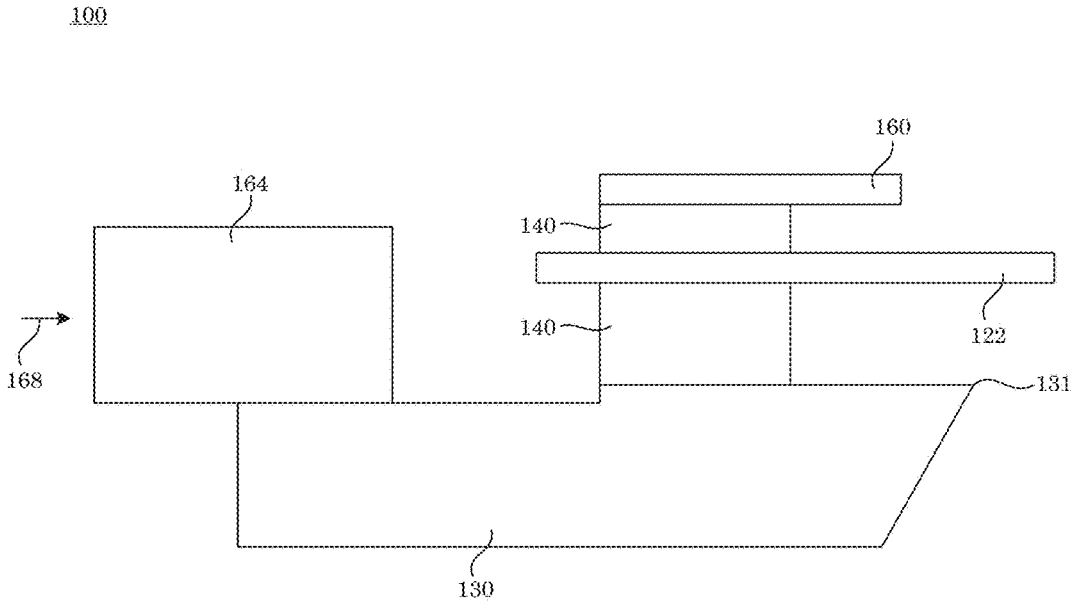

Figure 7

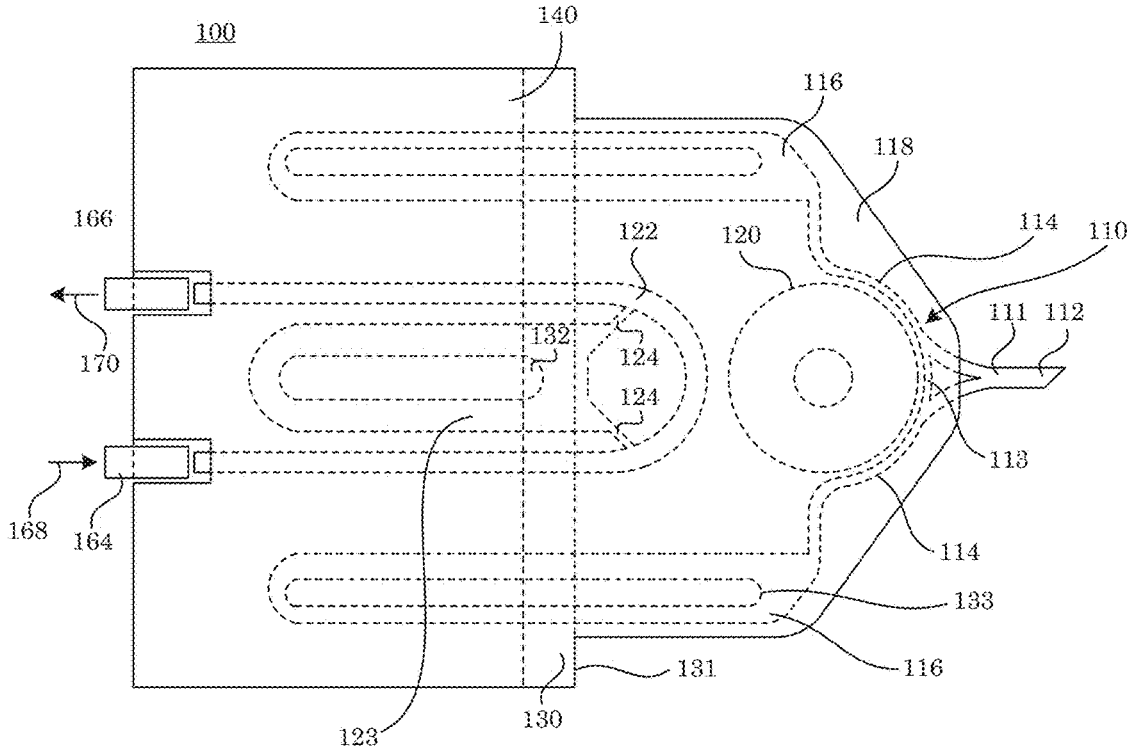
100
140
116
118
166
122
120
114
110
111
112
170
132
124
124
113
168
164
114
133
116
131
130
123

Figure 8

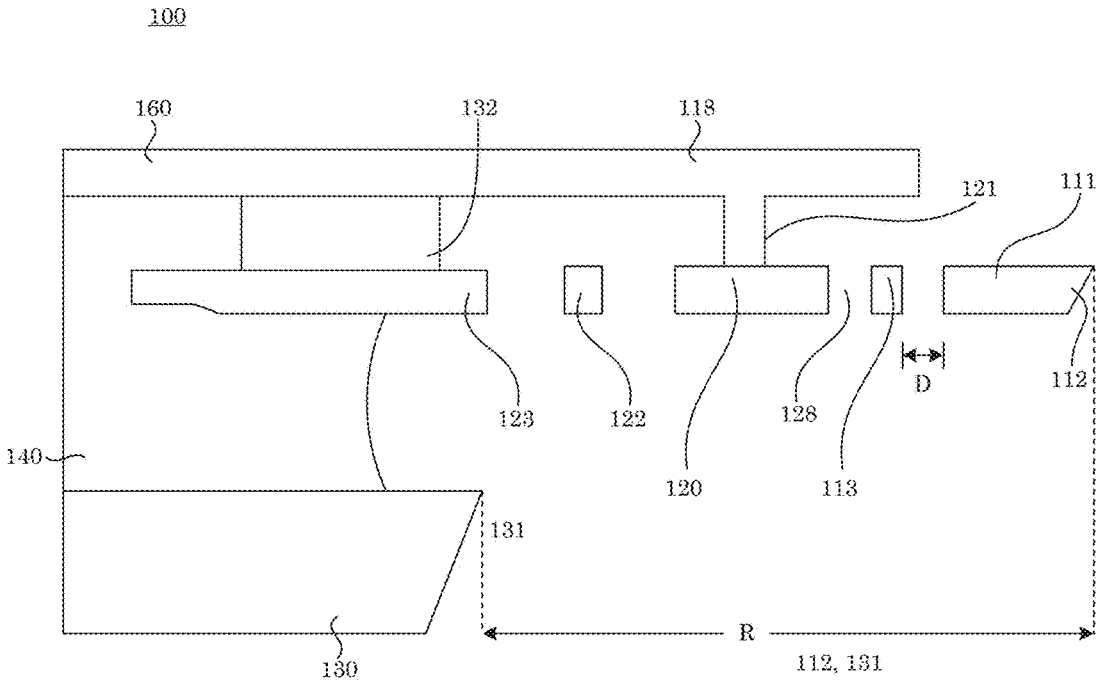
100
160
132
118
121
111
123
122
128
D
112
140
120
113
131
130
R
112, 131

Figure 9

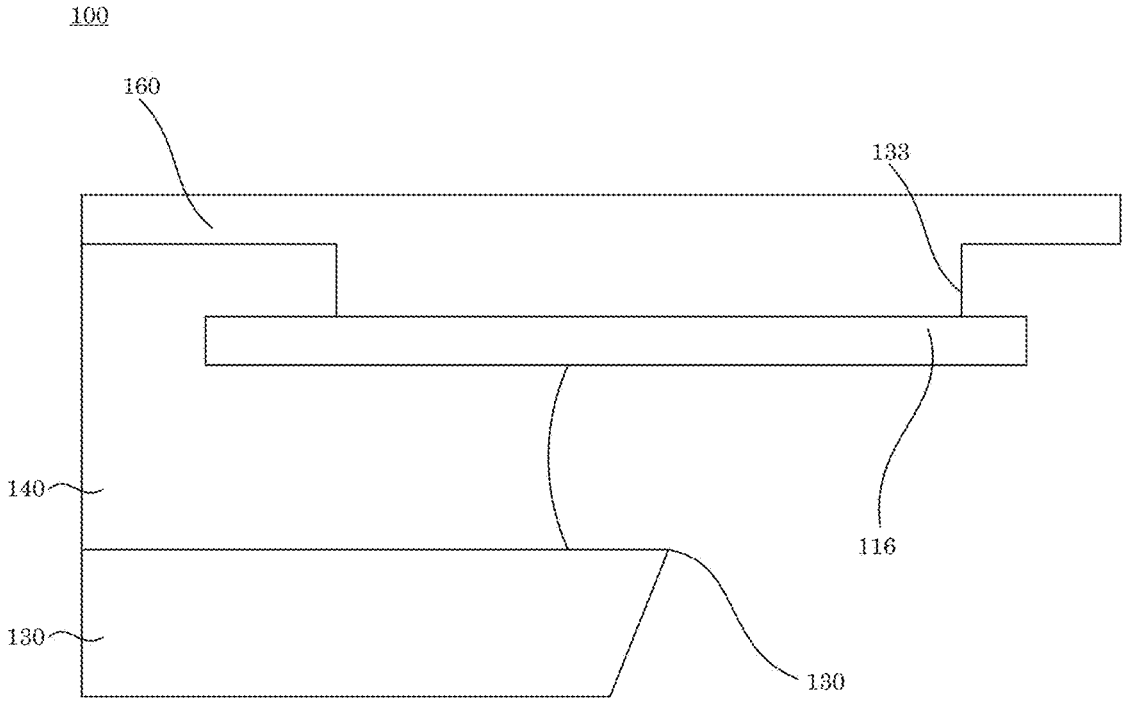

Figure 10

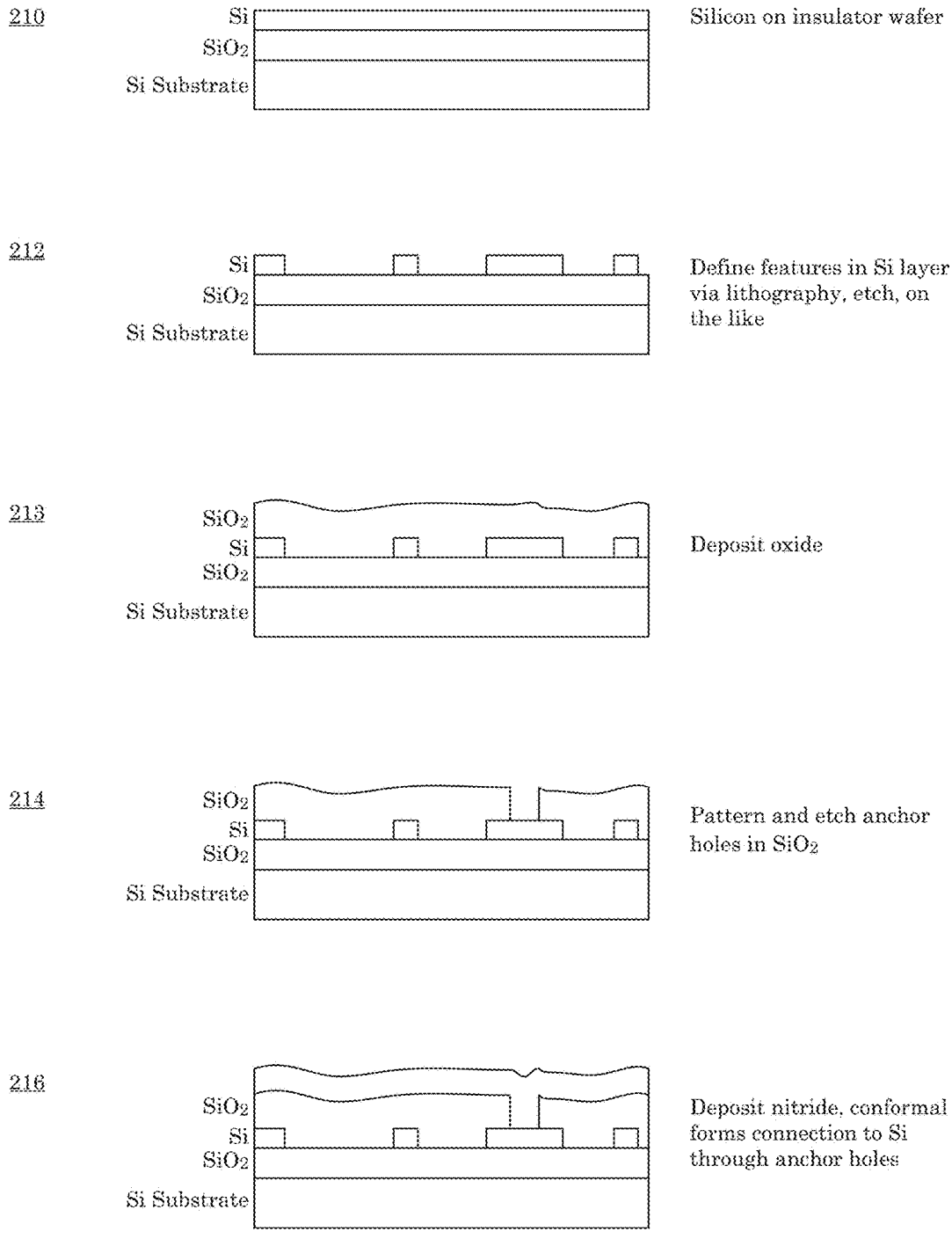
210
Si
SiO2
Si Substrate
Silicon on insulator wafer
212
Si
SiO2
Si Substrate
Define features in Si layer via lithography, etch, on the like
213
SiO2
Si
SiO2
Si Substrate
Deposit oxide
214
SiO2
Si
SiO2
Si Substrate
Pattern and etch anchor holes in SiO2
216
SiO2
Si
SiO2
Si Substrate
Deposit nitride, conformal forms connection to Si through anchor holes

Figure 11

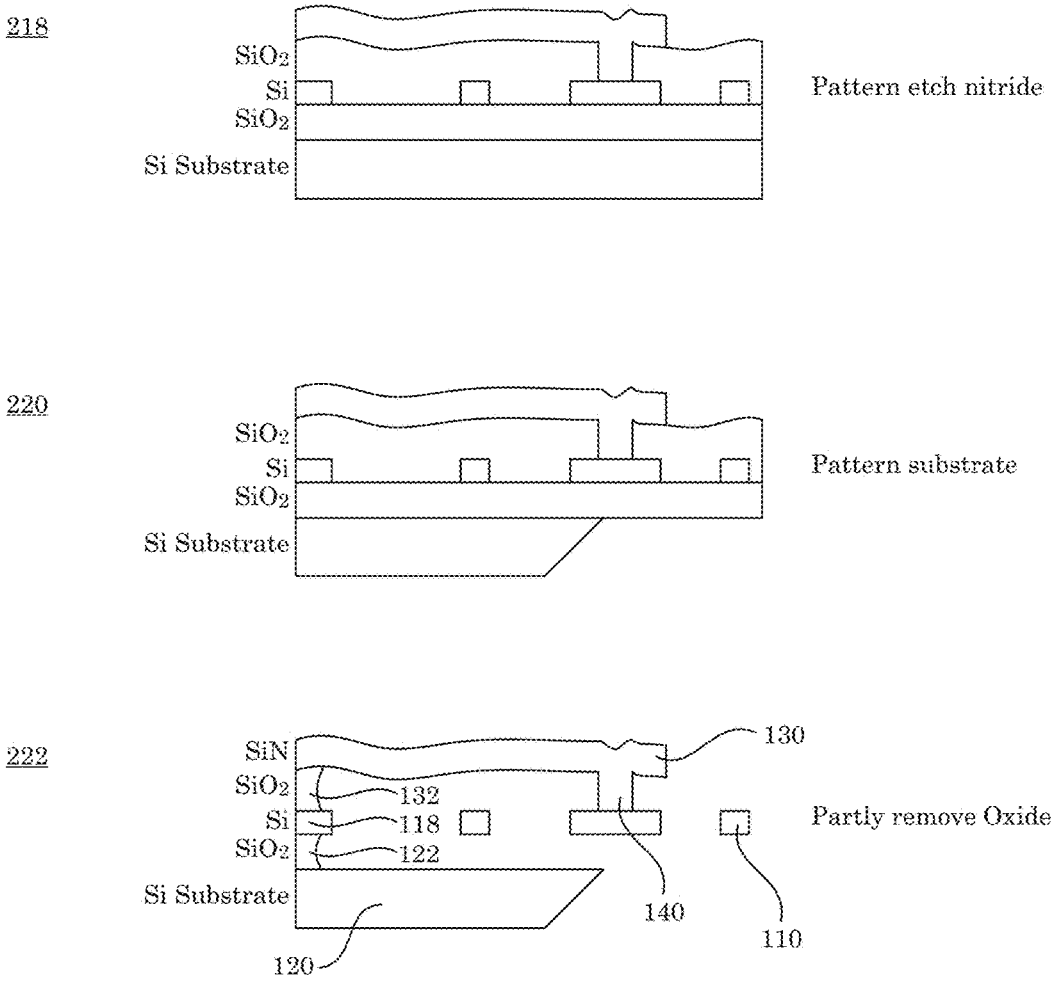
218
SiO2
Si
SiO2
Si Substrate
Pattern etch nitride
220
SiO2
Si
SiO2
Si Substrate
Pattern substrate
222
SiN
SiO2
Si
SiO2
Si Substrate
130
132
118
122
140
110
120
Partly remove Oxide

Figure 12

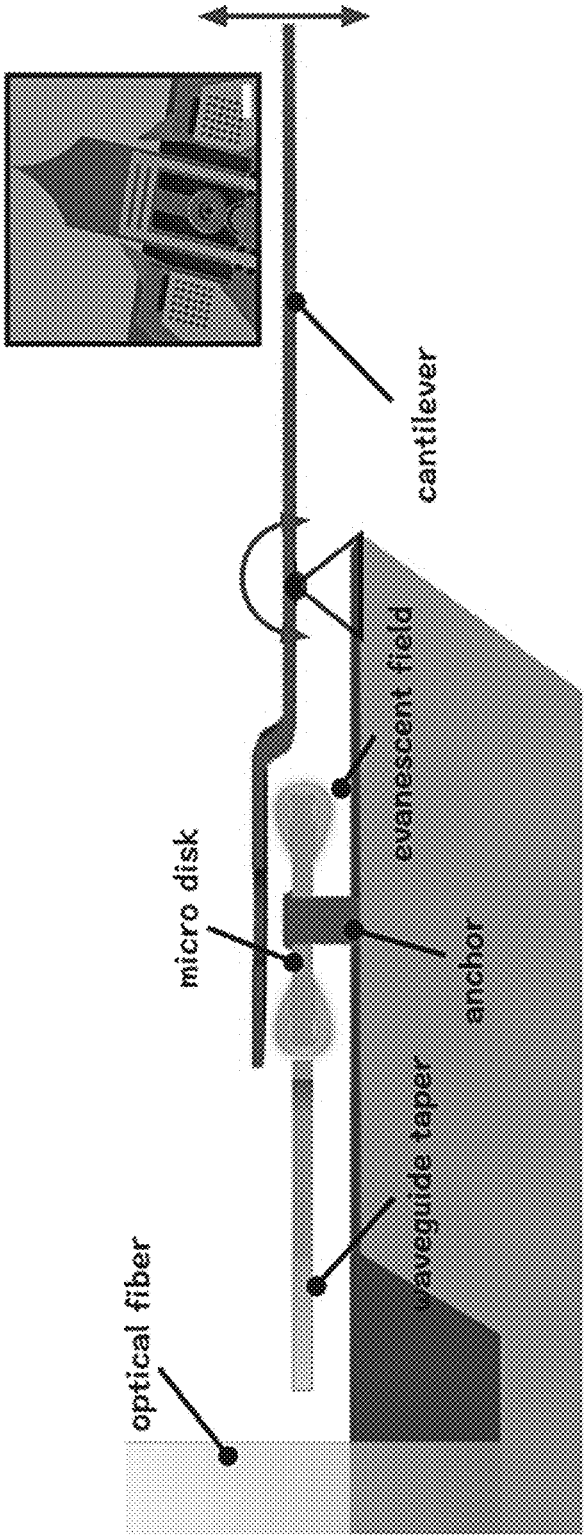
cantilever
evanescent field
micro disk
anchor
waveguide taper
optical fiber

Figure 13

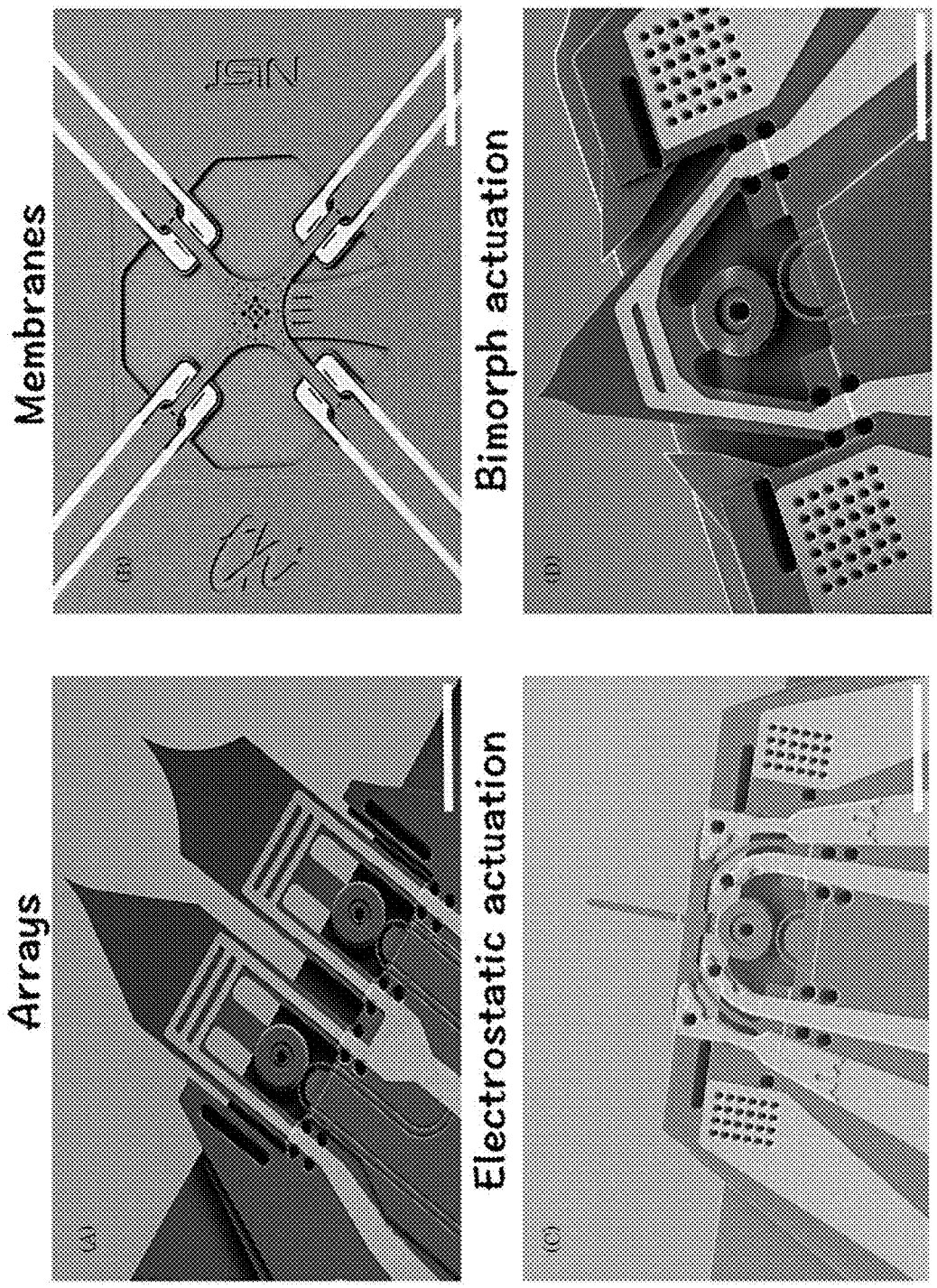
Arrays
Membranes
Electrostatic actuation
Bimorph actuation
(a)
(b)
(c)
(d)

Figure 14

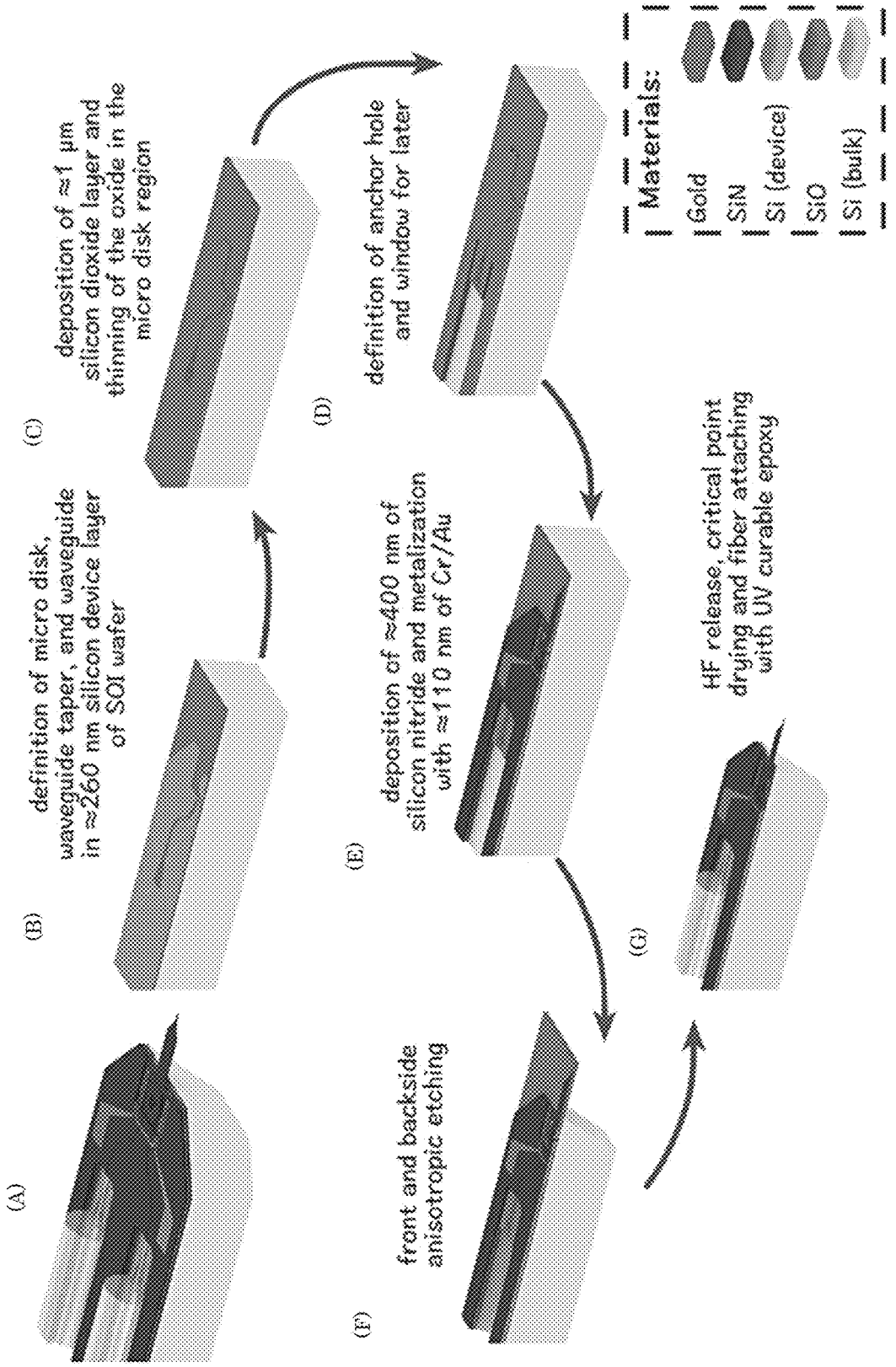
(A)
(B)
definition of micro disk, waveguide taper, and waveguide in ≈260 nm silicon device layer of SOI wafer
(C)
deposition of ≈1 μm silicon dioxide layer and thinning of the oxide in the micro disk region
(D)
definition of anchor hole and window for later
(E)
deposition of ≈400 nm of silicon nitride and metalization with ≈110 nm of Cr/Au
(F)
front and backside anisotropic etching
(G)
HF release, critical point drying and fiber attaching with UV curable epoxy
Materials:
Gold
SiN
Si (device)
SiO
Si (bulk)

Figure 15

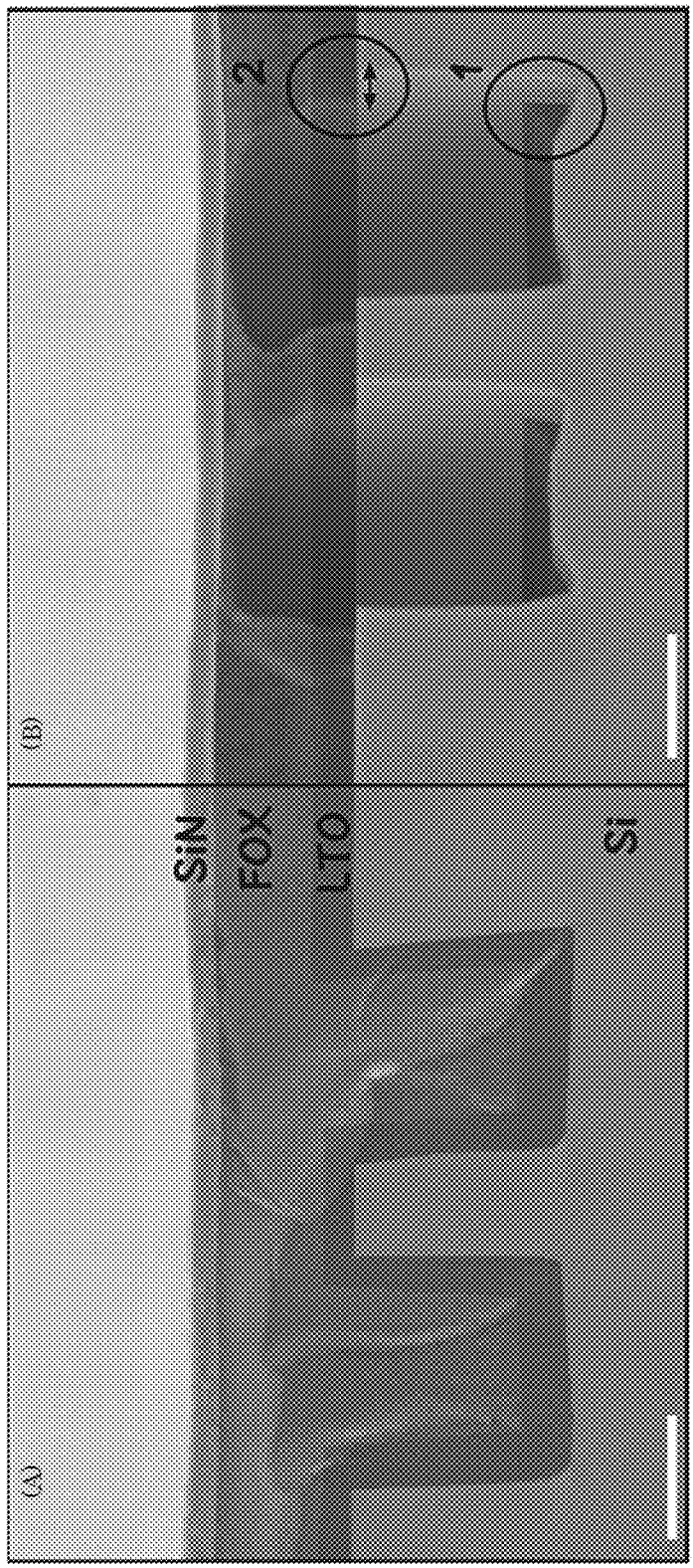

Figure 16

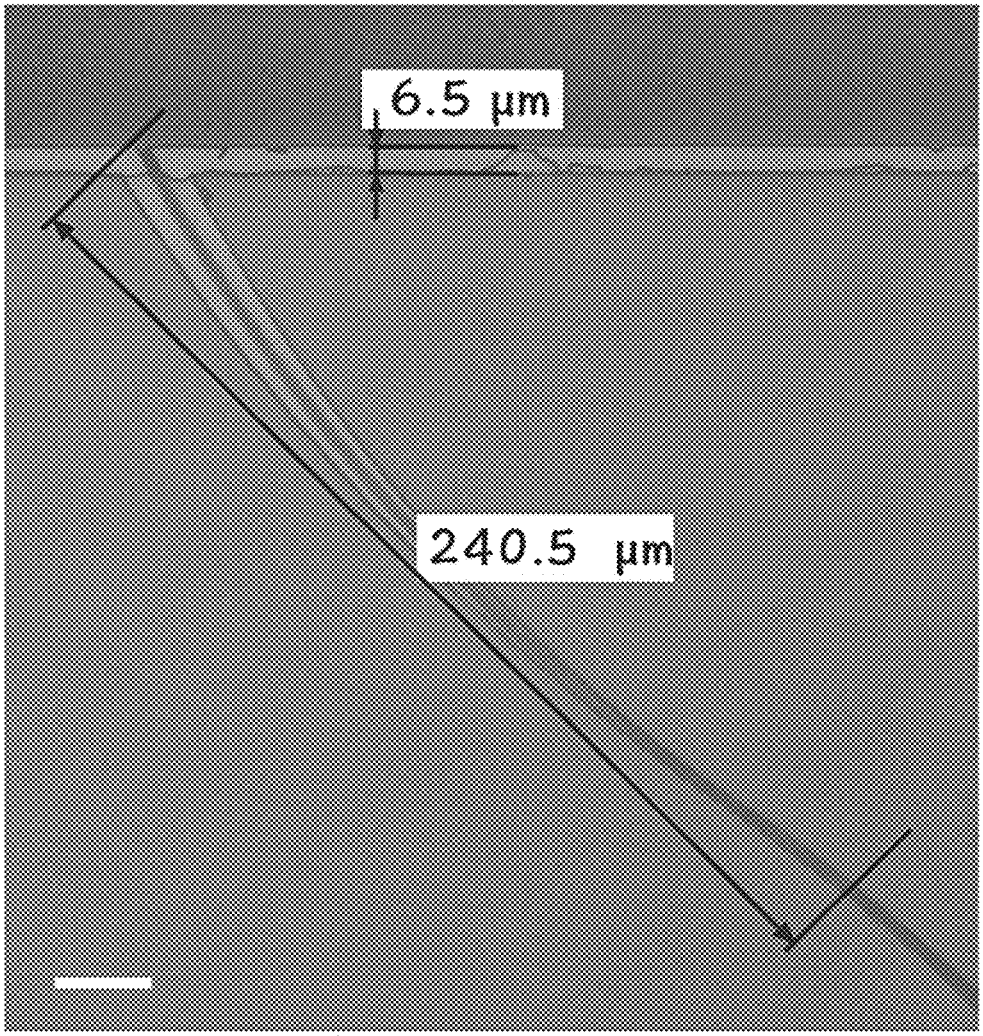

Figure 17

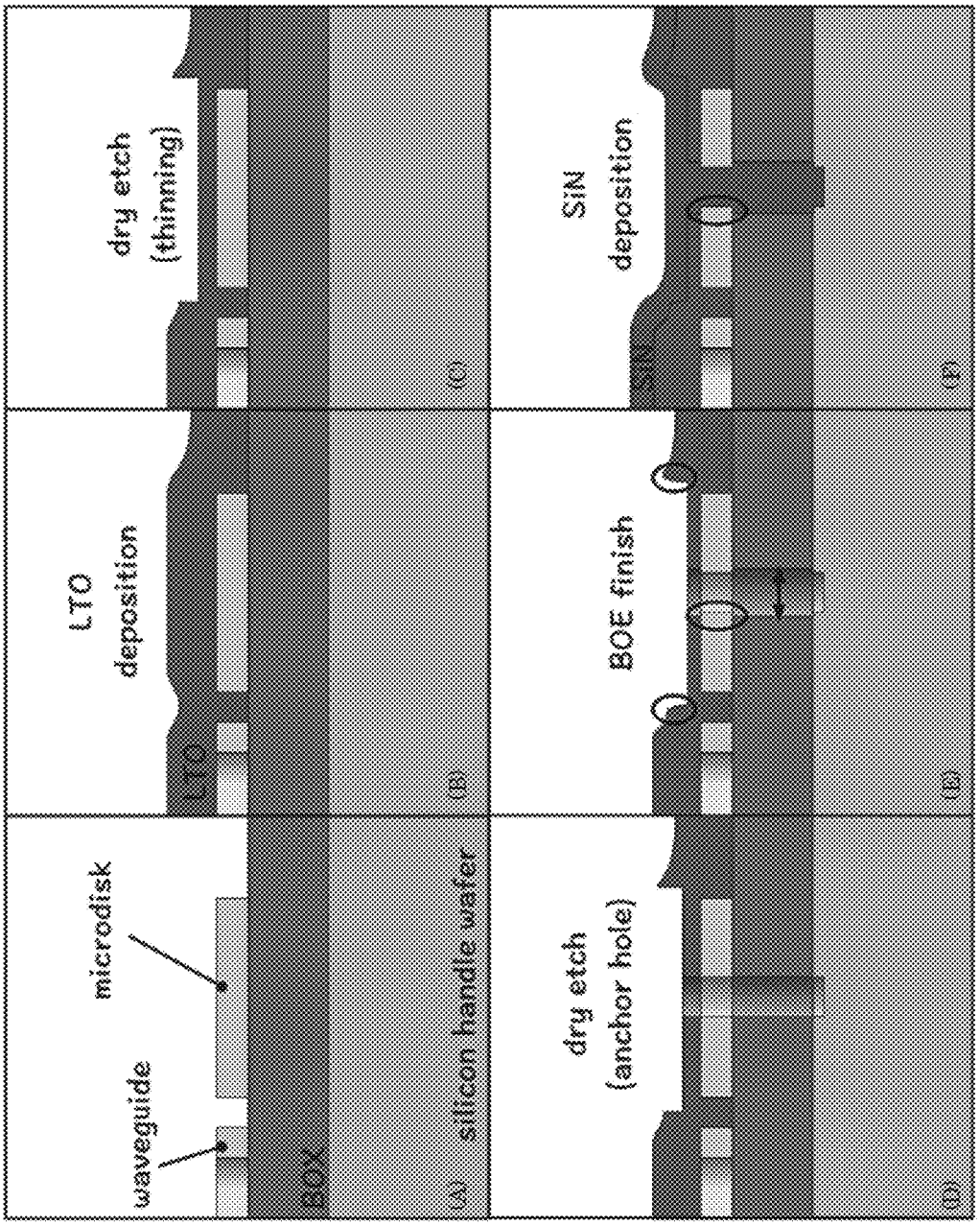
waveguide
microdisk
BOX
silicon handle wafer
(A)
LTO
LTO deposition
(B)
dry etch (thinning)
(C)
dry etch (anchor hole)
(D)
BOE finish
(E)
SiN
SiN deposition
(F)

Figure 18

PHOTONIC PROBE FOR ATOMIC FORCE MICROSCOPY

CROSS REFERENCE TO RELATED APPLICATIONS

This application claims the benefit of U.S. Provisional Patent Application Ser. No. 62/437,107, filed Dec. 21, 2016, the disclosure of which is incorporated herein by reference in its entirety.

This patent application is under obligation of assignment to the United States of America, as represented by the Secretary of Commerce. NIST has a proprietary interest in the application under 35 U.S.C. § 207.

STATEMENT REGARDING FEDERALLY SPONSORED RESEARCH

This invention was made with United States Government support from the National Institute of Standards and Technology (NIST), an agency of the United States Department of Commerce. The Government has certain rights in the invention. Licensing inquiries may be directed to the Technology Partnerships Office, NIST, Gaithersburg, Md., 20899; voice (301) 301-975-2573; email tpo@nist.gov.

BRIEF DESCRIPTION

Disclosed is a photonic probe for atomic force microscopy comprising: a cantilever comprising: a tip; a wing in mechanical communication with the tip; an extension interposed between the tip and the wing to synchronously communicate motion of the tip with the wing; an optical resonator disposed proximate to the cantilever and that: receives input light; and produces output light, such that: the cantilever is spaced by a gap distance from the optical resonator, wherein the gap distance varies as the cantilever moves relative to the optical resonator, and the output light differs from the input light in response to movement of the cantilever relative to the optical resonator; an optical waveguide in optical communication with the optical resonator and that: provides the input light to the optical resonator; and receives the output light from the optical resonator.

BRIEF DESCRIPTION OF THE DRAWINGS

The following descriptions should not be considered limiting in any way. With reference to the accompanying drawings, like elements are numbered alike.

FIG. **1** shows a top view of a photonic probe;

FIG. **2** shows a cross-section along line A-A of the photonic probe shown in FIG. **1**;

FIG. **3** shows a top view of a photonic probe;

FIG. **4** shows a top view of a photonic probe;

FIG. **5** shows a cross-section along line A-A of the photonic probe shown in FIG. **4**;

FIG. **6** shows a cross-section along line B-B of the photonic probe shown in FIG. **4**;

FIG. **7** shows a cross-section along line C-C of the photonic probe shown in FIG. **4**;

FIG. **8** shows a top view of a photonic probe;

FIG. **9** shows a cross-section along line A-A of the photonic probe shown in FIG. **8**;

FIG. **10** shows a cross-section along line B-B of the photonic probe shown in FIG. **8**;

FIG. **11** shows steps in a process for making a photonic probe;

FIG. **12** shows steps in a process for making a photonic probe;

FIG. **13** shows an exemplary schematic of the transducer (not to scale) showing overhung cantilever on a torsional pivot as the mechanical device. SiN is shown in green, Si is shown in blue and grey. The red arrow indicates the direction of movement. (inset) False-color scanning electron micrograph of a released device after the fabrication process. Yellow represents metallization, green represents SiN, light blue represents the Si device layer, and dark blue represents the Si handle wafer. Scale bar is 10 μm;

FIG. **14** shows designs of a process flow. The scale bars correspond to a) 20 μm, b) 100 μm, c) 30 μm, and d) 30 μm;

FIG. **15** shows a process flow for the transducer with integrated thermal actuation and overhanging tip. The image in the top left shows the finished device (a). (b) Definition of micro disk, waveguide taper, and waveguide in ≈260 nm silicon device layer of SOI wafer. (c) Deposition of ≈1 μm silicon dioxide layer in micro disk region. (d) Definition of anchor hole and window for later V-groove etching. (e) Deposition of ≈400 nm of silicon nitride and metallization with ≈110 nm of Cr/Au. (f) Front and backside anisotropic etching. (g) HF release, critical point drying and fiber attaching with UV curable epoxy;

FIG. **16** shows a cross sectional view of a test sample before (a) and after (b) the exposure to HF. The red circle in #1 points out that there is still LTO left in the corners of the trench, which shows that the lateral etch rate of the LTO is lower compared to the lateral etch rate of FOX in the trench. However, circle #2 shows that the lateral etch rates for both layers (LTO and FOX) are comparable outside the trench. This indicates that the high internal stress of the FOX layer in the trench has an influence on the lateral etch rate. The scale bars correspond to 400 μm;

FIG. **17** shows a top view of a cleaved test sample after the sample was exposed to HF for several minutes. The test sample consists of an SOI wafer structured with a waveguide. The waveguide structure is covered with a layer of LTO, FOX, and SiN. The images show a difference of lateral etch rate; and

FIG. **18** shows process steps for: a) after the transfer of the photonic structure, b) formation of the cladding layer, c) dry etch step of the thinning process, d) dry etch of the anchor hole, e) BOE finishing of the coupling region and shaping of the anchor hole, and f) SiN deposition.

DETAILED DESCRIPTION

A detailed description of one or more embodiments is presented herein by way of exemplification and not limitation.

Advantageously and unexpectedly, it has been discovered that a photonic probe for an atomic force microscope (AFM) includes an integrated photonic optomechanical cavity readout and provides high sensitivity, measurement speed, and low measurement noise for a variety of research and manufacturing metrology applications. The photonic probe has a compact mechanical and photonic element size with a tip that extends from a silicon chip edge and incorporates an optical resonator into a microfabricated overhanging mechanical cantilever that can include a photonic crystal or used microdisk cavity. Beneficially, the photonic crystal cavity is in a cantilever that is supported by a side of the cantilever structure.

In an embodiment, with reference to FIG. **1**, and FIG. **2**, photonic probe **100** for atomic force microscopy includes cantilever **110**. Cantilever **110** includes tip **112**; wing **114** in

mechanical communication with tip **112**; and extension **111** interposed between tip **112** and wing **114** to synchronously communicate motion of tip **112** with wing **114**. Wing **114** is flexible and provides motion of extension **111** and tip **112** relative to optical resonator **120**. Optical resonator **120** is disposed proximate to cantilever **110** and receives input light; and produces output light. Cantilever **110** is spaced by gap distance D from optical resonator **120**, wherein gap distance D varies as cantilever **110** moves relative to optical resonator **120**. Accordingly, the output light changes in response to movement of cantilever **110** relative to optical resonator **120**. Photonic probe **100** further includes optical waveguide **122** in optical communication with optical resonator **120**. Optical waveguide **122** provides the input light to optical resonator **120** and receives the output light from optical resonator **120**.

Cantilever **110** also includes proximal portion **113** disposed proximate to and spaced apart from optical resonator **120** by gap distance D. Distance D changes as tip **112** and extension **111** move toward or away from optical resonator **120** in response to interaction of tip **112** with a sample. Anchor **116** connects cantilever **110** to arm **118**. Arm **118** is disposed on substrate **130**. Additionally, connector **121** connects optical resonator **120** to arm **118**. Substrate **130** includes edge **131** that is spaced apart from a distal portion of tip **112** by recess R. Cover layer **160** is disposed on substrate **130**, wherein optical cladding **140** is interposed between cover layer **160** and waveguide **122** and between waveguide **122** and substrate **130**. Optical cladding **140** optically isolates the waveguide **122** from both the substrate **130** and the cover layer **160**. Moreover, a portion of arm **118** protrudes from edge **131** of substrate **130** and is exposed so that tip **112** can interact (e.g., physically contact) the sample, and a portion of arm **118** is disposed on optical cladding layer **140** such that optical cladding layer **140** mechanically attaches the arm **118** to the substrate **130**. Here, optical cladding layer **140** is interposed between arm **118** and both substrate **130** and covering layer **160**. Further, input optical fiber **164** receives input light **168** and communicates input light **168** to optical waveguide **122**. Optical waveguide **122** is in optical communication with optical resonator **120** and communicates input light **168** into optical resonator **120** and receives output light **170** from optical resonator **120**. Optical waveguide **122** communicates output light **170** to output optical fiber **166**. It should be appreciated that input light **168** can be the same or different than output light **170**, wherein the optical intensity, phase or both intensity and phase of the output light **170** are modified depending on the position and mechanical motion of the cantilever **110**. Here, optical resonator **120** includes a photonic crystal with the plurality of holes **128**. Holes **128** can be substantially identical sizes or different sizes. Holes **128** can be arranged in a one-dimensional array, a two-dimensional array, or a combination thereof. Either the hole size, their array period, or both size and period can be varied. Further, gap distance D can be uniform or nonuniform between cantilever **110** and optical resonator **120**, wherein a shape of the gap bounded by cantilever **110** and optical resonator **120** can be curved or straight.

In an embodiment of photonic probe **100**, with reference to FIG. **3**, input optical fiber **164** receives input light **168** and communicates input light **168** to optical resonator **120**. Optical resonator **120** receives input light **160** and outputs output light **170** based on interactions with cantilever **110**. Optical resonator **120** communicates output light **170** to output fiber **166**. It should be appreciated that cantilever **110** can have various shapes as shown in, but not limited by, FIG. **1** and FIG. **3**.

According to an embodiment, with reference to FIG. **4**, FIG. **5**, FIG. **6**, and FIG. **7**, photonic probe **100** includes optical resonator **120** that is a micro disc resonator. Micro disc resonator **120** is connected to arm **118** via connector **121**. Waveguide support **123** extends along substrate **130** and connects to optical resonator **120** via links **124**, **125**, wherein link **124** connects waveguide support **123** to optical waveguide **122**, and link **125** connects optical waveguide **122** to optical resonator **120**.

According to an embodiment, with reference to FIG. **8**, FIG. **9**, and FIG. **10**, waveguide support connector **132** is interposed between arm **118** and waveguide support **123**. Waveguide support connector **132** provides a rigid connection for arm **118** to waveguide support **123**. According to an embodiment, an anchor connector **133** is interposed between arm **118** and anchor **116**. Anchor connector **133** provides a rigid connection for arm **118** to anchor **116**.

In photonic probe **100**, substrate **130** provides a mechanical foundation for cantilever **110** and optical waveguide **122**. Exemplary materials for substrate **120** include silicon, glass, ceramic, sapphire, silicon carbide, or a combination thereof. In an embodiment, substrate **120** includes single crystal silicon. Additionally, the size of the substrate is selected such that it can be attached to the measurement instrument and to the optical fibers. The thickness of the substrate can be from 100 micrometers to 5 mm, and more specifically from 300 micrometers to 1 mm. In an embodiment, the substrate thickness is 600 micrometers. The substrate planar dimensions can be from 300 micrometers by 300 micrometers to 2 cm by 2 cm, more specifically from 1 mm by 3 mm to 1 cm by 1 cm. In an embodiment, the substrate dimensions are 5 mm by 5 mm. The substrate can be shaped as a rectangle, a square, a rectangle with cut corners or a rectangle with a protrusion on one side from which the cantilever protrudes.

Cantilever **110** is disposed on substrate **130** and protrudes such that it be brought into close proximity to a sample, whereby a local interaction with the sample modifies deformation or motion of the cantilever or both. The cantilever is disposed in proximity to the optical resonator **120** such that the cantilever motion modifies the optical properties of the optical resonator **120**. Exemplary materials for cantilever **110** include single crystal silicon, polycrystalline silicon, amorphous silicon, silicon nitride, diamond, silicon carbide, or a combination thereof. In an embodiment, cantilever **110** includes single crystal silicon. Additionally, the cantilever tip **112** may protrude a distance R from the substrate, where R is between 1 micrometer to 300 micrometers, more specifically between 10 micrometers and 100 micrometers. In an embodiment R is 20 micrometers. Additionally, the cantilever may be doped to increase electrical conductivity. Additionally, the cantilever may include surface coatings. It can be coated by materials such as diamond, or metals such as Cr, Au, Pt, Ag, Ti, W or a combination thereof.

Optical waveguide **122** is disposed on substrate **130** and transmits light from optical resonator **120**, to optical resonator **120** or both to and from the optical resonator **120**. Exemplary materials for optical waveguide **122** include single crystal silicon, polycrystalline silicon, amorphous silicon, silicon nitride, silicon carbide, diamond, high refractive index glass, transparent high refractive index polymer or a combination thereof. In an embodiment, optical waveguide **122** includes single crystal silicon. Additionally, the waveguide may be a single-mode waveguide.

Optical cladding layers **140** are disposed on substrate **130** and provides optical isolation of optical waveguide **122** from the substrate **130** and optical waveguide **122** from cover layer **160**. Exemplary materials for optical cladding layers **140** independently include silicon dioxide, glass, transparent polymer, or a combination thereof. In an embodiment, optical cladding layers **140** independently include silicon dioxide. Additionally, optical isolation depends on the effective refractive index of the guided mode and the thickness and refractive index of the cladding layers **140**. The thickness of the cladding layers **140** can be from 500 nm to 10 micrometers, more specifically from 1 micrometer to 3 micrometers. In an embodiment, the thickness is 2 micrometers. In another embodiment, the thickness is 1.5 micrometers.

Cover layer **160** is disposed on optical cladding layer **140** and provides protection of the cladding layer **140** during device fabrication, and provide a mask for selective removal of the cladding layer **140** during fabrication. Exemplary materials for cover layer **160** include silicon nitride, polymer, silicon, silicon carbide, aluminum nitride, chromium, chromium oxide, gold or a combination thereof. In an embodiment, cover layer **160** includes silicon nitride.

Arm **118** is connected to cover layer **160** and provides mechanical support, attaching the optical resonator **120** to substrate **130**. Exemplary materials for arm **118** include silicon nitride, silicon, silicon carbide, aluminum nitride, or a combination thereof. In an embodiment, arm **118** includes silicon nitride. In another embodiment, the arm **118** includes single crystal silicon.

Connector **121** is interposed between optical resonator **120** (e.g., the micro disc resonator) and arm **118** to provide mechanical support to the optical resonator **120**. Exemplary materials for connector **121** include silicon nitride, silicon, silicon carbide, aluminum nitride, or a combination thereof. In an embodiment, connector **121** includes silicon nitride. In another embodiment, the arm **118** includes single crystal silicon.

Optical fibers **164**, **166** are disposed on substrate **130** and connects input light **168** from an external apparatus to the waveguide **122** and to connect output light **170** from waveguide **122** to an external measurement apparatus. Exemplary materials for optical fibers **164**, **166** include doped glass and glass with air holes or a combination thereof. In an embodiment, optical fibers **164**, **166** independently include doped glass. Additionally, standard commercial telecommunications fibers and fiber cables can be used.

In an embodiment, with reference to FIG. **11** and FIG. **12**, a process for making photonic probe **100** includes providing substrate **130** (step **210**), wherein a layer of silicon dioxide or silicon can be disposed thereon as in a silicon on insulator wafer; defining features in the silicon layer, e.g., via lithography, etching, and the like (step **212**); depositing an oxide on the silicon layer (step **213**); patterning and etching holes in the oxide layer (step **214**); depositing in nitride conformally to form a connection to silicon through the holes (step **216**); patterning and etching the nitride layer (step **218**); patterning substrate **130** (step **220**); and partially removing the oxide to form photonic probe **100** (step **222**).

According to an embodiment, a process for probing a sample includes attaching a source of input light **168**, such as a tunable laser, to the input fiber **164**, attaching the output fiber **166** to the detection apparatus, such as a photodiode, to detect the output light; tuning the input light frequency on resonance of optical resonator **120**, more specifically on the shoulder of the absorption line of the optical resonator **120**, whereby the motion of the cantilever changes the optical resonance frequency and modulates intensity of the output light **170** in proportion to the displacement of the cantilever **110** and in proportion changes the output voltage of the detection apparatus; approaching the tip **112** to a sample until the cantilever moves and the transmitted light is modified; scanning the tip **112** along the sample surface while recording the output light using the detection apparatus. The measurement process may further include modifying the distance between sample and probe **100** in a periodic and aperiodic fashion, including by application of feedback; inducing motion of the cantilever **110** by applying electrostatic force, shaking the substrate **130** or providing stimulation with a laser; and using changes in the detected output light **170** to infer various characteristics of the interactions of cantilever tip **112** and the sample, including sample height, elastic properties, time and spatially dependent forces and force gradients, including conservative and dissipative forces between the tip **112** and the sample and such.

Photonic probe **100** and processes herein have numerous advantageous and unexpected properties. Unexpectedly, the probe can simultaneously have small mass from 5 pg to 0.2 pg, and have low motion detection noise spectral density from 10 fm/Hz^0.5 to 0.1 fm/Hz^0.5. The small mass probe can advantageously have high first mechanical mode frequency from 1 MHz to 150 MHz and thereby can respond quickly to mechanical stimuli and rapid changes in its interaction with the sample, while at the same time can have a low to modest stiffness from 0.1 N/m to 100 N/m. Such stiffness is advantageous for a variety of measurements that avoid excessive sample damage, yet allow accurate control of probe-sample separation. Rapid probe response is advantageous for measuring rapidly time-dependent and transient interactions and for completing measurements quickly, while at the same time the advantageously low motion-detection noise allows to make these measurements precisely. Furthermore, the unexpected combination of small size and low motion-detection noise results in reduced measurement noise in air and liquid environment, advantageously allowing more precise and faster atomic force microscopy in such environments.

Moreover, in some embodiment, optical resonator **120** overhangs substrate **130** and connects to cantilever **110**. Cantilever **110** can be mechanically supported by attachment to substrate **130** on one side such that one end of cantilever **110** partially overhangs substrate edge **131**. In this manner, a length of cantilever **110** can be longer than extension **112** and optical cavity **120** sizes and provides a tolerance for placing substrate edge **131** during manufacturing.

Further, optical resonator **120** can include a photonic crystal or micro disc resonator. With the photonic crystal, optical resonator **120** can be mechanically supported from a side of the photonic crystal without loss of optical quality. The photonic crystal cavity is formed at an end of a cantilever overhanging the substrate. The photonic crystal evanescently interacts with a cantilever that includes the tip and includes a small mode volume for strong interaction with the cantilever. The photonic crystal can be mechanically interconnected with the cantilever and disposed on the substrate via the optical cladding layer. In some embodiments, the substrate is absent. Instead of precisely machining the edge of the substrate, the edge of the substrate can be machined or formed using less rigorous methods. Moreover, the cantilever can be made of a same planar material layer that the optical cavity is made of, wherein the material includes a single crystal silicon film layer.

In another embodiment, the cantilever can be formed by micromachining techniques from an additional layer of material such as a film of silicon nitride deposited on top of the layer that includes the optical resonator. For the optical resonator that includes the micro disc cavity, the micro disc cavity can be mechanically attached to the cantilever at a center of the micro disc cavity by a mechanical anchor attached to a central portion of the microdisk cavity. The cantilever can be spatially separated from the optical fields at the microdisk edge, such as by using and removing sacrificial material of sufficient thickness during formation of the cantilever to preserve optical quality. Forming the anchor and using sacrificial layers are techniques for surface micromachining.

An optical quality factor of the photonic probe can be greater than two million at an optical wavelength 1557 nm, with optomechanical coupling 5 GHz/nm, mechanical stiffness 1.5 N/m, and effective mass 0.9 pg.

Advantageously, the photonic crystal can be coupled to and interrogated evanescently by integrated, fiber-coupled photonic waveguides. Also, the optical waveguide can be incorporated into a two-dimensional photonic crystal or a one-dimensional photonic crystal. The photonic crystal and cantilever extend beyond and overhang the edge of the substrate.

The photonic probe with integrated optical resonator is useful for atomic force microscopy and provides high sensitivity, fast and reliable measurement speed, low measurement noise for research and manufacturing metrology applications. The compact mechanical and photonic element sizes and the ability to attach photonic resonator to an overhung cantilever overcome previous difficulty of manufacturing of conventional probes designs due to absence of demanding tolerances for precise undercutting of the substrate edge to expose the probe tip but mechanically anchor the center of the microdisk optical resonator to the arm.

The articles and processes herein are illustrated further by the following Example, which is non-limiting.

EXAMPLE

This Example describes batch fabrication of a fiber pigtailed optomechanical transducer platform with an overhanging member. The platform provides a high bandwidth, high sensitivity, and highly integrated sensor that is compact and robust with the potential for low cost batch fabrication inherent in micro-opto-electro-mechanical-systems (MEMS) technology.

The fabrication process includes electron beam lithography, i-line stepper lithography, and back- and front-side mask aligner lithography. Moreover, this process makes use of equipment in nanofabrication facilities and research laboratories, facilitating broad adaptation and application of the process. Therefore, this process is useful for the nano- and microfabrication research communities at large.

An obstacle to realizing the potential of micro- and nanomechanical sensing is the readout of the motion of the small resonator with high sensitivity, high bandwidth, and without excess power dissipation. In the past years numerous methods for the readout of resonator motion have been developed. Electrical readout schemes, such as capacitive, magnetomotive, piezo-resistive, and piezoelectric are convenient but suffer from various combinations of poor scaling with reduced size, power dissipation limitations, magnetic field and material requirements, and thermal Johnson noise in the readout signal. On the other hand, optical readout schemes, such as beam deflection and interferometric, substitute optical shot noise for thermal noise, in principle don't dissipate any power at the transducer, and have a high measurement bandwidth. However, to effectively couple motion to light, most of the off-chip optical methods need a certain minimum moving structure size and reflectivity, which often involves bulky structures or mechanically dissipative reflective coatings.

In nanophotonic optical cavities, light is trapped in a very small volume and interacts for a longer time and more closely with the mechanical resonator. Typical photonic cavity optical quality factors on the order of 10^5 to 10^6 increase the readout signal-to-noise by the same factor. The readout bandwidth is reduced from ≈100 THz optical frequency to about ≈100 MHz, still fast enough for most mechanical sensors. Maintaining stable coupling of a microscopic mechanical resonator with an off-chip optical cavity is challenging due to alignment and drift of components with respect to each other. Here this challenge is overcome by integrating the high-quality factor optical cavity directly underneath the moving device, allowing strong interaction with the optical near-field of the cavity, while avoiding mechanical contact (FIG. **13**). This interaction is described by the optomechanical coupling coefficient (g_{OM} typically in the units of GHz/nm) relating the change in optical frequency of the micro disk cavity to the displacement of the mechanical device. This fully integrated stable and practical optomechanical transducer is fiber connectorized and implements the readout of mechanical motion with gigahertz bandwidth.

Low-loss, stable, and robust fiber coupling of the transducer provides sensitive and reliable operation. Therefore, the fibers are securely attached to the chip without excess losses between the on-chip waveguide and the optical fiber.

This readout approach provides independent tailoring of the various optical and mechanical parts of the transducer. The photonics can be separately optimized for low losses, high quality factor and desired cavity size, while tuning the waveguide-cavity coupling depth and the optomechanical coupling to achieve the optimal readout sensitivity and dynamic range. The mechanical components' size, shape, stiffness, and resonance frequency can be tailored to best address the specific sensing applications. The actuation can be tailored for the displacement and force ranges, ideally without introducing mechanical losses, avoiding increased mechanical noise and decreased Q in resonators.

Conventional devices focus on parts of a transducer, e.g., tuning of optical cavities coupling to optical chips, displacement measurement on moveable structures, or the fundamental physics of optical microdisk cavities. Here, a compact, robust fiber pigtailed optomechanical transducer platform is described, which is useful for the nanofabrication and nanophotonic research community, and process steps can be adapted for other fabrication projects.

FIG. **13** shows an arrangement of components in our transducer platform that includes an optical fiber, inverse-taper coupler, waveguides, microdisk cavity, and the mechanical (torsional cantilever) structure. Electrically-controlled actuators (not shown) are also included in the platform to tune the static position and dynamically excite the motion of the mechanical device.

The photonic structures for operation in the telecommunication wavelength range (≈1550 nm) are fabricated in the silicon device layer of a silicon-on-insulator (SOI) wafer, because of the outstanding optical and mechanical properties of silicon. The mechanical device is created in silicon nitride (SiN), because it shows good mechanical properties resulting in high quality factor devices, has low optical loss, an

index of refraction below that of Si and is compatible with a hydrofluoric (HF) acid release. For the metallization, we choose gold with a chromium adhesion layer (Cr/Au), compatible with HF and potassium hydroxide (KOH) etches. Furthermore, the combination of SiN and Cr/Au shows a good thermal bimorph actuation efficiency. Silicon dioxide is used as the sacrificial material.

The sensitivity to motion is proportional to the optical quality factor of the micro disk cavity and quickly increases with decreasing gap between the cavity and the mechanical resonator. It is therefore important to accurately locate the mechanical structure in close proximity to the optical micro disk cavity, while maintaining the high optical quality ($\approx 10^5$ to $\approx 10^6$) factor of the micro disk optical mode. In our design, the micro resonator is lithographically aligned to the disk, and completely encloses it, while a sacrificial layer defines the gap in the fabrication process. A dedicated lithography step and an etch step are used to reduce the sacrificial layer thickness to a predetermined value at the optomechanical transducer (≈400 nm), allowing us to control the gap within tens of nanometers, while keeping a thicker silicon dioxide sacrificial and cladding layer elsewhere. The thickness has been determined with simulations and measurements. It is important that the gap between the silicon microdisk and the silicon nitride is not too small, to avoid excessive leakage form the optical mode into the silicon nitride layer. This would dramatically reduce the optical quality factor of the device. Furthermore, for some of the transducers presented in this paper, discussed in other papers, it is possible to tune the readout gain.

Separating photonic and mechanical layers affords flexibility in the design of the mechanical parts to suit specific sensing applications. Within the same process flow, we design and fabricate mechanical cantilever structures, torsional structures, and membranes, on chip structures, and overhanging structures, as well as various types of actuation mechanisms (FIG. **14**). The transducer arrays can be used for the simultaneous high sensitivity force detection, such as in parallelized scanning probe microscopy. The membrane transducers show a high mechanical quality factor and good frequency stability, which can be used to study forces acting on samples attached to the membrane. Four different designs of the membrane transducer are designed to have resonance frequencies between ≈70 kHz and ≈2 MHz. The two different option for excitation of the photonic probes allow to design probes with a high-quality factor and stable resonance frequency as well as probes with tunable readout gain. The cantilever probes show resonance frequencies between ≈50 kHz and ≈2 MHz for the first eigenmode.

The integration of an actuator increases the range of possible applications. The built-in static actuation allows tuning the transducer gain and measurement range. This is accomplished by changing the static gap size between the mechanical structure and the optical cavity. We decided to develop designs for two actuation schemes, thermal bimorph and electrostatic actuation. Bimorph actuators deliver fast responses and large forces. However, the introduction of metal on the mechanical structure creates significant internal losses and therefore reduces the mechanical quality factor. In contrast, electrostatic fringe field actuation does not involve metal in contact with the mechanical member, which lets the mechanical member freely oscillate and does not affect the mechanical quality factor. This commonly used type of actuation enables measurements on dielectric resonators, where useful electrostatic forces for frequency tuning and motion excitation are applied directly to the dielectric structure, thus avoiding any unwanted degradation of the mechanical quality factor.

The devices were fabricated in a unified batch fabrication process and a single platform, which can be tailored for specific applications. In the following we will present the process using the overhanging cantilever probe.

The fabrication of the cavity optical transducer is based on double-side polished SOI. The process flow is summarized in FIG. **15**. In the first step, the waveguide taper, waveguide, and micro disk are defined via electron beam lithography and inductively-coupled reactive ion etching (RIE) of the SOI device layer down to the buried oxide layer (BOX). The nominal width of the waveguide is ≈500 nm and the gap between the waveguide and the disc is defined to be ≈340 nm. Both waveguide ends are linearly tapered down to a width of ≈100 nm over the distance of ≈50 μm for low loss coupling to/from optical fibers (≈5.5 dB per facet) (FIG. **15***b*). The remaining structures are defined by i-line stepper optical lithography unless otherwise noted. A sacrificial silicon dioxide layer (≈1 μm) is deposited in a low-pressure chemical-vapor deposition furnace (LPCVD) and defined to create a window to the Si substrate for the later KOH etching as well as a hole in the center of the micro disk, which is used to anchor the micro disk to the bulk silicon with the following SiN layer. The silicon dioxide is thinned down by a CF_4 plasma etch through a lithographically-defined window in photoresist in the region above the micro disk to ensure good optomechanical coupling (FIG. **15***c, d*). The optomechanical coupling for these devices is ≈26 GHz/nm. A low-stress silicon nitride layer (≈400 nm) deposited with LPCVD acts as a passivation layer in the waveguide region and as a structural material for the mechanical structure. Following nitride deposition, a gold layer is deposited and defined in a liftoff process to create a micro heater, electrical connection, and wire bond pads. For the electrostatically actuated transducer, the micro heater is replaced by electrodes for fringe field actuation. The SiN layer is lithographically patterned (FIG. **15***e*), and dry etched to form the SiN cantilever, SiN ring above the micro disk, and SiN anchor to mechanically attach the micro disk to the bulk silicon. The previously defined metal layer is used as a hard mask for SiN, to self-align the SiN structure in critical areas (FIG. **15***e*). For front side protection during the later KOH etch, a hafnium oxide (HfO) layer is deposited with atomic layer deposition. In the following, a RIE is used to open up a window in the HfO and SiN for anisotropic etching of the silicon, and to form v-grooves for optical fibers. A back to front aligned backside lithography followed by RIE etching is used to form an anisotropic etch window on the backside as well. Both lithographies for the definition of the front and back side etch window for anisotropic etching are defined with contact aligner lithography. During the anisotropic silicon etch, V-grooves are formed on the front side of the chip and the shape of the cantilever chip is defined by etching through the handle wafer from the backside (FIG. **15***e*). Another approach is the replacement of the backside KOH etch with an ICP etch to create a backside trench with vertical sidewalls. This approach is currently being used to develop acceleration sensors with large seismic masses made from the handle wafer.

Silicon dioxide layers and HfO are removed by 49% HF wet etching to undercut and release the movable structures as well as the micro disk, which is anchored to the bulk silicon with a SiN anchor. A critical point drying process is used to avoid stiction between the parts due to capillary forces (FIG. **15***f*). At the end of each v-groove the over-

hanging waveguide inverse tapers are suspended between silicon support structures and coupled to optical fibers. Which are placed in the V-groove, actively aligned and glued into place with ultraviolet (UV) light curable epoxy.

The described fabrication process is based on a 100 mm SOI wafer. The device layer thickness of the wafer is ≈260 nm with low doping to insure good optical transmission. The buried oxide layer has a thickness of ≈2 μm, which is important to prevent leakage of the optical energy in the guided mode from the photonic structure into the silicon handle wafer. The crystal orientation in the handle wafer and the device layer is (100) which results in the desired V-groove and cantilever chip shape after the anisotropic etching.

For backside polishing, the fabrication starts with polishing the backside of the SOI wafer for better control of the anisotropic backside etching as one of the final fabrication steps. The polishing is achieved with a table-top chemical mechanicals-polishing system (CMP). For the protection of the front side of the wafer during the polishing process, a combination of a silicon dioxide hard mask and a soft mask created with photoresist is used. The hard mask is created with a flowable oxide (i.e., FOX 16). The flowable oxide is based on an inorganic polymer in a methyl isobutyl ketone (MIBK) carrier solvent, the solvent volatilizes rapidly from the resin, leaving a planar surface. The soft mask consists of a thick photoresist mask.

For cleaning: the wafer is cleaned with N-Methyl-2-pyrrolidone (Resist remover 1165) at ≈70° C. for ≈15 min, followed by a rinse with isopropyl alcohol and blow dry with nitrogen gun. Alternatively, the wafer can be dried in the spin dryer and is useful for batch fabrication runs with more than one wafer.

For frontside protection including a hard mask, "FOX 16" diluted ≈1:10 with MIBK is used for the hard mask; the FOX is applied with the following spin coater setting of ≈10.47 rad/s (≈100 rpm) for ≈5 s followed by ≈314.16 rad/s (≈3000 rpm) for ≈40 s, and the mask is cured in three consecutive soft bake steps to prevent the layer from cracking. Starting with ≈90° C. for ≈1 min, followed by ≈180° C. for ≈1 min, and ≈400° C. for ≈1 min, resulting in a cured thickness of ≈400 nm.

For frontside protection a soft mask is used in which: the soft mask is created with a thick photo resist layer ("AZ 10xT") with the following spin coater parameter of ≈10.47 rad/s (≈100 rpm) for ≈5 s followed by ≈209.44 rad/s (≈2000 rpm) for ≈45 s, and the polymer layer is cured in a soft bake step of ≈115° C. for ≈10 min, resulting in a cured thickness of ≈12 μm.

For chemical mechanical polishing (CMP), a slurry solution based on colloidal silica ("Ultra-Sol 556") diluted with deionized water in a ratio of ≈4:10 is used for the polishing process; the process steps for the conditioning of the system are summarized below, and for the conditioning of the polishing pad, the "Conditioner" is lowered on our CMP system. The conditioning step is used to break in the polishing pad for reproducible results. The steps and conditions are as follows

Step #1
- Time: 5 min
- Force: 2.5 kg
- Pump #1: 0 ml/min (Slurry)
- Pump #2: 40 ml/min (H_2O)
- Pad: ≈4.7 rad/s (≈45 rpm) (CW)
- Wafer: 0 rad/s (0 rpm)
- Slider: 50 mm to 70 mm (5 min^{-1})

Step #2
- Time: 5 min
- Force: 2.5 kg
- Pump #1: 50 ml/min (Slurry)
- Pump #2: 0 ml/min (H_2O)
- Pad: ≈4.7 rad/s (≈45 rpm) (CW)
- Wafer: 0 rad/s (0 rpm)
- Slider: 50 mm to 70 mm (5 min^{-1})

After conditioning, the conditioner is raised to allow the wafer/polishing pad contact; the following parameters are chosen to polish the backside of the wafer down to a polished surface. This polishing step removes ≈20 μm of material on the rough wafer backside of a single-side polished wafer.

Step #1
- Time: 1 min
- Wafer: 100 mm
- Force: 17.236 kN/m^2
- Pump #1: 20 ml/min (Slurry)
- Pump #2: 0 ml/min (H_2O)
- Pad: ≈3.66 rad/s (≈35 rpm) (CW)
- Wafer: ≈3.14 rad/s (≈30 rpm) (CCW)
- Slider: 50 mm to 70 mm (10 min^{-1})

Step #2
- Time: 2 h+30 min
- Wafer: 100 mm
- Force: 45.642 kN/m^2
- Pump #1: 20 ml/min (Slurry)
- Pump #2: 0 ml/min (H_2O)
- Pad: ≈3.66 rad/s (≈35 rpm) (CW)
- Wafer: ≈3.14 rad/s (≈30 rpm) (CCW)
- Slider: 50 mm to 70 mm (10 min^{-1})

Step #3
- Time: 15 min
- Wafer: 100 mm
- Force: 3.447 kN/m^2
- Pump #1: 0 ml/min (Slurry)
- Pump #2: 50 ml/min (H_2O)
- Pad: ≈3.66 rad/s (≈35 rpm) (CW)
- Wafer: ≈3.14 rad/s (≈30 rpm) (CCW)
- Slider: 50 mm to 70 mm (5 min^{-1})

The slurry should not sit on the wafer for a long time after the polishing finished because the slurry will attack the surface. To avoid an attack of the surface, the wafer is rinsed thoroughly with DI water right after the polishing to remove all slurry residues and dried with nitrogen.

For cleaning, the wafer is cleaned with N-Methyl-2-pyrrolidone (Resist remover 1165) at ≈70° C. for ≈15 min, followed by a rinse with isopropyl alcohol and deionized water DI water (DIW) dump rinse; buffered oxide etch (16% BOE) is used for the removal of the hard mask. This etch is performed in cycles of 30 s of etching and a DI water dump rinse until the silicon surface is hydrophobic. This step takes ≈1 min for the described oxide thickness. Before the start of the patterning processes, the wafer is cleaned using the Radio Corporation of America cleaning (RCA clean). Table 1 lists the parameters for cleaning.

TABLE 1

RCA I	
Solution:	DIW/NH_4OH/H_2O_2(50 ml/10 ml/10 ml)
Time:	≈10 min
Temperature:	≈75° C.

TABLE 1-continued

HF dip	
Solution:	HF/DIW (2 ml/100 ml)
Time:	≈30 s
Temperature:	room temperature (RT)
RCA II	
Solution:	DIW/HCl/H_2O_2(50 ml/10 ml/10 ml)
Time:	≈10 min
Temperature:	≈75° C.

For this step, the wafer was placed in a 100-mm cassette for the handling; add the hydrogen peroxide only a few minutes before the cleaning; otherwise, the hydrogen peroxide will be consumed by the bath before the actual cleaning. The hydrogen peroxide for RCA II should not be added earlier then ≈7 min before the bath is used.

The wafers are dump rinsed between every step. After the last cleaning bath, the wafers are dried in the spin dryer. A good test during the cleaning is to check the hydrophobicity of the silicon surface after the HF dip. The surface should be hydrophobic, if this is not the case, the HF dip should be repeated.

Alignment marks were made according to the following step that includes electron beam lithography. We use the flat of the wafer to align the wafer to the electron beam lithography layer to the crystallographic orientation of the silicon wafer. For the alignment of the electron beam lithography, we create alignment marks with a contact mask aligner and a silicon etch on the wafer. We then use these alignment marks to actively align the lithography pattern written by the electron beam system to the crystal orientation of the wafer. The alignment marks are also used for drift check during the electron beam write, to minimize stitching between the write fields. The depth of these alignment marks is very important to create a mark with good contrast in the electron beam tool. The alignment marks are lithographically defined in an i-line stepper lithography.

For lithography, hexamethyldiloxane is used for the preparation of the wafer surface to improve the adhesion between resist and wafer surface; the wafer is heated up in a vacuum furnace to ≈120° C.; after a short bake-out (≈20 min), Hexamethyldiloxane vapor is flowed into the chamber for the deposition, followed by a couple of purge cycles to remove the Hexamethyldiloxane from the chamber prior to venting to atmosphere; a standard positive photoresist is used for this lithography process ("S1813"), and the resist layer is applied in a spin coating process, with the following spin speed parameters of ≈10.47 rad/s (≈100 rpm) for ≈5 s followed by ≈418.88 rad/s (≈4000 rpm) for ≈45 s (final resist layer thickness ≈800 nm). The resist is soft baked at ≈115° C. for ≈1 min. The wafer is exposed with 140 mJ/cm^2 (I-line 365 nm) at 365 nm with a focus of 0 μm, numerical aperture of 0.6, and a sigma of 0.7 in the "annular" illumination mode.

For pattern transfer, the structure is transferred with a parallel plate reactive ion etcher; the silicon device layer is etched with a sulfur hexafluoride chemistry, followed by an etch based on fluorocarbon chemistry for the silicon oxide layer (the BOX layer of the SOI wafer), and the parameters of the etch are summarized in Table 2.

TABLE 2

Si Etch	
Tool:	RIE #2
Time:	3 min
Gases:	SF6/CF4
Flow rates:	≈6 mL/min (≈6 sccm)/≈24 mL/min (≈24 sccm)
Pressure:	≈1 Pa (8 mTorr)
RF power:	≈200 W
Ref. RF power:	≈0 W
DC Bias:	≈516 V
Etch rate:	≈100 nm/min
SiO_2 etch	
Tool:	RIE #2
Time:	12 min
Gases:	O2/CHF3
Flow rates:	5 mL/min (5 sccm)/45 mL/min (45 sccm)
Pressure:	6.7 Pa (50 mTorr)
RF power:	200 W
Ref. RF power:	≈0 W
DC Bias:	≈516 V
Etch rate:	≈35 nm/min

The depth of the final marks was more than 750 nm to be clearly visible in the electron beam lithography system.

For cleaning, after the dry etch, the wafer is cleaned in a piranha solution (H_2SO_4:H_2O_2) to remove the resist as well as the polymers which have been created during the etch process. A piranha solution with the ratio H_2SO_4:H_2O_2 (3:1) is used. The wafers are placed in the fresh solution for ≈10 min, followed by a dump rinse and spin dry.

For electron beam lithography, this step defines the photonic structures in the silicon device layer. The nominal width of the final waveguide is ≈500 nm and the gap between the waveguide and the disk is defined to be ≈340 nm. The waveguide is linearly tapered down to a width of ≈100 nm over the distance of ≈50 μm at both waveguide ends for low loss coupling to optical fibers. All dimensions are positively biased by 10 nm for the electron beam lithography to take dimension change due to oxidation into account. We use the electron beam resist "ZEP 520A" with a base dose of ≈460 μC. The base dose is modulated to compensate proximity effects in the lithography process, which is critical for the disk/waveguide gap as well as for the waveguide taper width. Small variations in these dimensions have a significant effect on the optical device performance. The electron beam lithography is performed on a gaussian beam electron beam system with a write field of 1 mm^2.

The structures are written with "floating" write fields to optimize the lithography results. "Floating" fields are primarily used to eliminate stitching in critical areas. Floating field pattern fracturing forces the field stitch boundaries to known areas, which are typically chosen to contain straight sections of a waveguide. Additionally, the layout and pattern conversion are optimized to reduce the writing time between consecutive fields containing stitched elements. This reduces any drift induced stitching errors. The resist is developed with hexyl acetate at ≈0° C. to improve the contrast, followed by a transfer step for the generated pattern into the silicon device layer. We transfer the pattern with a hydrogen bromide and chlorine chemistry (HBr/Cl_2). This etch was chosen as it is known to be a highly anisotropic silicon etch with good control over the sidewall angle. HBr also produces fewer defects in the surface. Alternatively, we tried a pseudo gas-chopping approach with a plasma chemistry based on octafluorocyclobutane and sulfur hexaflouride (C_4F_8/SF_6). The lithography step combined with the transfer into the silicon device layer is a critical step in this fabrication process, since a small deviation in the created lateral

device dimension can have a significant influence on the optical performance of the devices.

For the electron beam lithography, the resist "ZEP 520A" is used because of its good selectivity in our silicon etch process (An alternative product is "CSAR62"). The resist is applied with a spin coater and the following spin speeds of ≈10.47 rad/s (≈100 rpm) for ≈5 s followed by ≈366.52 rad/s (≈3500 rpm) for ≈35 s, which results in a final layer thickness of ≈400 nm). The resist is soft baked at ≈180° C. for ≈2 min. To minimize charging effects during the electron beam lithography, a thin charge dissipation layer based on ≈15 nm of aluminum is used. This thin metal layer has a negligible influence on the electron beam resolution but shows a sufficient conductivity to reduce charging of the resist. Furthermore, aluminum can be easily removed with tetramethylammonium hydroxide (TMAH) based developer after the exposure. The aluminum layer is applied via thermal evaporation. The evaporation with a source based on electron beam heating might affect the resist properties due to unwanted exposure to electron beams.

For the exposure of the prepared wafer, an electron beam lithography tool is used, with a base dose of ≈460 After the exposure, the aluminum layer is removed in TMAH based developer ("MF319") for less than 1 min. Shortly after dipping the exposed sample into the developer, the exposed area will appear in the aluminum layer, before the aluminum layer starts to disappear. The wafer is rinsed with DIW to remove residuals of the developer and dried with nitrogen. The wafer electron beam resist is developed in hexyl acetate at ≈0° C. to improve the contrast. A cooling plate based on Peltier elements is used to achieve a sufficient temperature control. The development in cold hexyl acetate takes ≈120 s. The wafer is removed from the developer and dried with nitrogen immediately to remove developer residuals. Alternatively, the wafer can be rinsed with MIBK and isopropyl alcohol (IPA) before dying. However, MIBK can create cracks in "ZEP 520A" with a thickness of more than about ≈400 nm.

Before the pattern can be transferred into the silicon device layer, the chamber is conditioned for the etch chemistry. Depending on the starting conditions, this sometimes takes more time than mentioned in this recipe. The conditioning starts with a bare 100 mm silicon wafer, which is etched for ≈20 min. After the etching, the wafer surface should be shiny and not dark black. The shiny surface is a good indicator that the chamber is clean and in reasonable condition. A black surface indicates the creation of black silicon on the wafer, which is an indicator that the chamber condition is not ideal. Table 3 provides the conditions for conditioning.

TABLE 3

Tool:	Plasma etcher
Time:	≈20 min
Substrate:	≈100 mm silicon wafer
Gases:	HBr/Cl_2
Flow rates:	≈10 ml/min (≈10 sccm)/≈5 ml/min (≈5 sccm)
ICP power:	≈700 W
Ref. ICP power:	≈6 W
RF power:	≈60 W
Ref. RF power:	≈1 W
Pressure:	≈2 Pa (≈15 mTorr)
Temperature:	≈20° C.
Helium backing:	≈2.6 Pa (≈20 Torr)
DC Bias:	≈155 V

The conditioning with the bare silicon wafer is followed by a silicon wafer with resist pattern. The exposed silicon area of this wafer is approximately the area which will be etched on the process wafer as well. The only difference is, that this is a bare silicon wafer with a resist mask created via stepper lithography, to create waveguide structures for visual inspection of the etch results. Further conditioning parameters are included in Table 4.

TABLE 4

Tool:	Plasma etcher
Time:	≈2 min 30 s
Substrate:	≈100 mm silicon wafer with resist mask
Gases:	HBr/Cl_2
Flow rates:	≈10 ml/min (≈10 sccm)/≈5 ml/min (≈5 sccm)
ICP power:	≈700 W
Ref. ICP power:	≈6 W
RF power:	≈60 W
Ref. RF power:	≈1 W
Pressure:	≈2 Pa (≈15 mTorr)
Temperature:	≈20° C.
Helium backing:	≈2.6 Pa (≈20 Torr)
DC Bias:	≈142 V

The etch results are inspected in the scanning electron microscope to determine the sidewall angle, etch rate, and uniformity across the wafer. Typical sidewall angles are between ≈90° and ≈87°. The typical etch rate is ≈95 nm/min with an etch rate uniformity of ±5 nm in lateral dimension. The sidewall angle can be adjusted with the process pressure. The test etch is repeated until the desired etch profile is reached. Pattern transfer conditions are listed in Table 5.

TABLE 5

Tool:	Plasma etcher
Time:	adjusted with results from test etch
Substrate:	≈100 mm SOI wafer with ZEP 520A
Gases:	HBr/Cl_2
Flow rates:	≈10 ml/min (≈10 sccm)/≈5 ml/min (≈5 sccm)
ICP power:	≈700 W
Ref. ICP power:	≈6 W
RF power:	≈60 W
Ref. RF power:	≈1 W
Pressure:	≈2 Pa (≈15 mTorr)
Temperature:	≈20° C.
Helium backing:	≈2.6 Pa (≈20 Torr)
DC Bias:	≈142 V

The structure is over etched to create vertical sidewalls across the whole wafer and compensate for possible non-uniformities in the vertical etch rate. The displayed DC Bias will change if the surface of the buried oxide layer is reached. The etch rate of the resist is ≈72 nm/min. An over etch into the BOX layer is acceptable as the etch rate on silicon oxide is ≈50 times higher than that of silicon.

Another commonly used etch chemistry for photonic structures is an ICP etch based on sulfur hexafluoride and octafluorocyclobutane. In contrast to the standard gas chopping process, where these gases are used in alternating steps of "etching" (sulfur hexafluoride) and "passivating" (octafluorocyclobutane), they are used simultaneously instead to create very smooth sidewalls. However, this simultaneous etching and passivation makes the process difficult to use because of a small process window for a stable etch. The rate at which the passivation is deposited on the side wall and bottom of the trench strongly depends on the chamber conditions, i.e., polymers build-up on the chamber walls. We were able to realize devices with similar optical quality

factors with this etch chemistry. However, the process strongly depends on the etch load and the chamber conditions and therefore has to be adjusted for every sample. This makes this etch preparation very time consuming. Furthermore, this etch is very sensitive to over etching. During an over-etch, BOX layer will charge up, which creates a deflection of the ions at the bottom. These defected ions etch the sidewall passivation and create notching.

In contrast to this, an over-etch with the HBr chemistry does not create notching because the anisotropic properties of the etch are not created by a side wall passivation. The vertical side walls depend on the directional kinetic energy of the HBr radicals. The etch is based on the amporphization effect of Cl_2 and HBr on silicon.

The wafer is cleaned with a combination of solvents to remove the plasma baked resist after the etching. In the first step, a solvent based on N-Methylpyrrolidone and N-(2-Hydroxyethyl)-2-Pyrrolidone ("EKC-Remover") at ≈70° C. for ≈10 min, followed by a dump rinse and spin dry. Piranha solution (H_2SO_2:H_2O_2) is used to remove the bulk polymer in a ratio of H_2SO_2:H_2O_2 (3:1) for ≈10 min followed by a dump rinse and spin dry.

The electron beam lithography is followed by an i-line stepper lithography to define larger-area structures in the silicon device layer. This step defines a trench around the cantilever chip and removes the silicon device layer below the future cantilever structure. The stepper lithography uses a standard positive photoresist and is followed by an inductive plasma etch process to transfer the structure into the silicon. The HBr chemistry has been chosen for this step because of the high etch selectivity between silicon and silicon dioxide. The stepper lithography and the earlier electron beam lithography overlap in certain areas to create continuous regions with removed silicon. The high etch selectivity reduces the step between the two areas, which is created in the this etch process.

The wafer is exposed with 140 mJ/cm^2, a focus of 0 μm, a numerical aperture of 0.6, and a sigma of 0.7 in the "angular" illumination mode. The pattern is developed in "MF 319" for ≈60 s followed by a DIW rinse and dried with nitrogen.

The pattern is transferred with the HBr recipe described above. Table 6 provides pattern transfer conditions.

TABLE 6

Recipe:	Plasma etcher
Time:	adjusted with results from test etch
Substrate:	≈100 mm SOI wafer with resist mask
Gases:	HBr/Cl_2
Flow rates:	≈10 ml/min (≈10 sccm)/≈5 ml/min (≈5 sccm)
ICP power:	≈700 W
Ref. ICP power:	≈6 W
RF power:	≈60 W
Ref. RF power:	≈1 W
Pressure:	≈2 Pa (≈15 mTorr)
Temperature:	≈20° C.
Helium backing:	≈2.6 Pa (≈20 Torr)
DC Bias:	≈142 V

The structure is over etched by 10% to ensure uniform results.

The wafer is cleaned with piranha solution (H_2SO_2:H_2O_2) to remove the bulk polymer as well as etch residuals. A ratio of H_2SO_2:H_2O_2 (3:1) is used for ≈10 min.

For waveguide cladding and spacer layer, the waveguide cladding layer consists of silicon dioxide. The cladding is created in a thermal oxidation and a chemical vapor deposition (CVD) step where low temperature oxide (LTO) is deposited. A first thermal oxidation step is used to clean the silicon surface from any contamination, as well as defects created during the silicon etch. This clean will also remove the halogenated and amphorizied surface layer, which has been created by Cl_2 and HBr during the silicon etch. The created oxide is removed with a wet oxide etch followed by a second thermal oxidation. The second thermal oxidation creates a good interface layer between the silicon crystal and the silicon dioxide layer created by CVD. Unfortunately, the thickness of the oxide layer created by our deposition tool has a non-uniformity of ≈±10%. To reduce the influence on the deposited layer, the deposition process is split into three separate depositions. The wafer is turned between the depositions by ≈120°. After the first LTO deposition, the layer is etched back with a silicon dioxide dry etch to prevent the creation of encapsulated cavities in the oxide due to the growth dynamics of the CVD process. The dry etch is based on a tetrafluoromethane (CF_4) chemistry, because this chemistry creates fewer etch residuals. This is important to avoid any contaminations of the cladding layer. This step is followed by two LTO depositions and a high temperature anneal in a nitrogen atmosphere. The annealing process drives the hydrogen out of the layer and improves the mechanical, electrical, optical, and chemical (etch rate) properties. The N_2 atmosphere prevents a further oxidation of the silicon device layer.

Before the deposition of the cladding layer, the wafer is cleaned with a RCA clean. The wafer is cleaned.

For thermal oxidation, the SOI wafer is placed with one clean bare monitor silicon wafer on each side in the furnace boat. The monitor wafers are used to determine the grown silicon dioxide thickness after the run. The wafers are dry oxidized at ≈1000° C. for ≈10 min, which will create an oxide thickness of ≈12 nm. Therefore, the original silicon surface is moved ≈5 nm into the silicon, since the volume of thermal oxide consists out of ≈44% silicon. The wafers are removed from the furnace and the oxide is stripped in diluted HF (≈2%), followed by a dump rinse and spin dry. The wafer is etched in diluted HF until the surface is hydrophobic. The thermal oxidation can be repeated with the same or similar parameters

For LTO deposition or for the CVD deposition, we determined the deposition rate with a full wafer boat and on the wafers in the center of the boat. The non-uniformity in this process between wafers can be significant. The wafers in the center are in general more uniform then wafers on the sides of the boat. The SOI wafer is placed in the center of the boat with one clean monitor silicon wafer on each side. The monitor wafers are used to determine the grown silicon dioxide thickness after the run. The deposition is performed at ≈400° C. for ≈400 nm. The wafers are removed and etched in a parallel plate reactive ion etcher, the parameters are listed in Table 7.

TABLE 7

Tool:	RIE Unaxis 790
Depth:	≈200 nm
Gases:	O2/CF4
Flow rates:	≈5 sccm/≈25 sccm
Pressure:	≈6.7 Pa (≈50 mTorr)
RF power:	≈200 W

After the etch back, the wafers are loaded into the CVD furnace for the next LTO deposition. The deposition is again performed at ≈400° C. for ≈400 nm. The wafers are rotated to improve the uniformity of the deposition, followed by the

last deposition. The deposition is performed at ≈400° C. for ≈600 nm. After the final deposition, the wafers should have a final silicon dioxide thickness of ≈1.2 μm. To finish up the LTO deposition, the wafers are annealed at ≈1000° C. in a N_2 atmosphere for ≈1 h. The annealing process drives the hydrogen out of the layer and improves the mechanical, electrical, optical, and chemical (etch rate) properties. The N_2 atmosphere is very important to prevent a further oxidation of the silicon device layer.

As alternate approach to creating a cladding, use FOX as described previously for the polishing hard mask. The advantage of FOX is the outstanding planarization capability, which will level all topographical steps and therefore simplify the lithographies for the following fabrication steps. In addition, the processing time for FOX compared to the LTO deposition is lower and less expensive. FOX is applied in a spin coating process and soft baked on a hot plate, followed by a rapid thermal annealing (RTA) and a 1 h annealing in a nitrogen atmosphere. However, we observed problems with FOX as waveguide cladding for this process. The silicon waveguide is defined by a trench, with an aspect ratio of (1:2), on each side. In test experiments, we cured the FOX layer with different temperatures and atmospheres and were able to create a planar layer without any visible defects or cracks. However, if we released test chips with trench structures in HF, we observed a much higher lateral etch rate for the oxide in the trench compared to the oxide elsewhere. To rule out any effects originating from the interface between the silicon and the oxide cladding we introduced a thin silicon dioxide layer (created with LTO) as interface layer. FIG. **16** shows the cleaved cross section of the test structure before (left) and after the HF etch (right). The red circle #1 points out that there is still LTO left in the corners of the trench, which shows that the lateral etch rate of the LTO is lower compared to the lateral etch rate of FOX in the trench. However, circle #2 shows that the lateral etch rates for both layers (LTO and FOX) are comparable outside the trench. This suggests that the high internal stress of the FOX layer in the trench has an influence on the lateral etch rate. Since no defects are visible in the optical microscope and scanning electron microscope, we assume that the stress creates nanometer size cracks along the trench which allow a significant increase of the etch rate in HF along the trench. FIG. **17** shows a top view of an etch SOI wafer with trench structure, LTO, FOX, and SiN. The difference in the etch rates is clearly visible. We can see an etch rate of 160 nm min^{-1} on the planar surface and 4800 nm min^{-1} in the trench.

Another indicator for nanometer size cracks along the trench was found in a second etch experiment with BOE. BOE is known to attack silicon dioxide, but due to a different surface tension it doesn't creep into narrow cracks. The second etch experiment shows a significantly smaller difference between the lateral etch rate in the trench and on planar surface.

The gap between the silicon micro disk and the mechanical member (i.e., cantilever or membrane) is important for the optical performance of the transducer. For smaller gaps, the optomechanical coupling increases exponentially. However, a smaller gap also decreases the optical quality factor of the disk due to increased loss of optical energy from the disk mode into the silicon nitride structure. Simulations show that a reasonable value for the gap is ≈400 nm. Therefore, to reach this value the cladding layer on top of the micro disk has to be thinned down to ≈400 nm. Furthermore, an anchor point is created to hold the photonic structures in place after the final removal of the silicon dioxide sacrificial layer. To improve the future anchor point of the micro disk and the transition, between the area with the thick LTO cladding and a thinner LTO layer on top of the disk, a combination of dry etching and wet oxide etching is used. The dry etch creates a step profile in the oxide and the wet etch is used to round the corners of this step profile as well as undercut the silicon micro disk around the future anchor point. FIG. **6** shows these process steps in detail.

A bottom antireflective coating (ARC) is used to decouple the optical properties of the sample from the lithography process. The correct thickness of this layer is essential for its functionality. A standard ARC used for this process is "AZ BARLi-II" with a final thickness of ≈180 nm. This is achieved with the spin coat parameter summarized below. The ARC is followed by a layer of positive photo resist ("SPR 220-3"). A resist thickness of ≈1.2 μm has been chosen, because it supplies enough resist for the etch processes as well as good coverage of all topographical steps. The process parameters are summarized in table 8.

TABLE 8

Resist layer 1: BARLi II	
Spin speed:	≈10.5 rad/s (≈100 rpm) for ≈5 s/≈209.4 rad/s (≈2000 rpm) for ≈40 s
Soft bake:	≈200° C. for ≈60 s
Resist layer 2: SPR 220-3	
Spin speed:	≈10.5 rad/s (≈100 rpm) for ≈5 s/≈314.2 rad/s (≈3000 rpm) for ≈40 s
Soft bake:	≈115° C. for ≈90 s

The wafer is exposed with 190 mJ/cm^2, a focus of 0.4 μm, a numerical aperture of 0.48, and a sigma of 0.5 in the "conventional" illumination mode. The resist is treated with a post exposure bake, of ≈110° C. for ≈60 s, to improve the result of the lithography process. In the following, the structure is developed in "AZ 300 MIF" for ≈60 s followed by a DIW rinse and dried with nitrogen.

The transfer process starts with a long descum to remove the ARC at the bottom of the lithographically defined structures. The used oxygen plasma etch only removes the organic part of the ARC; the inorganic part will be removed in the following etch based on tetrafluoromethane chemistry. The etch step with tetrafluoromethane chemistry is also used to thin the oxide cladding layer in the region above the disk to a final thickness of ≈600 nm (FIG. **18***c*). The process parameters are summarized in the table 9, and the etch is performed in a parallel pate reactive ion etcher.

TABLE 9

Descum	
Tool:	RIE
Time:	≈7 min
Gases:	O_2/Ar
Flow rates:	≈5 ml/min (≈5 sccm)/≈20 ml/min (≈20 sccm)
Pressure:	≈4 Pa (≈30 mTorr)
RF power:	≈50 W
Ref. RF power:	≈0 W
SiO2	
Depth:	until a final cladding thickness of ≈600 nm above the silicon disk is reached
Gases:	O2/CF4
Flow rates:	≈5 ml/min (≈5 sccm)/≈25 ml/min (≈25 sccm)
Pressure:	≈6.7 Pa (≈50 mTorr)
RF power:	≈200 W

The wafers are cleaned with a combination of solvents and acids to remove the plasma baked resist after the etching as well as the ARC. The first step of the cleaning is a solution based on N-Methyl-2-pyrrolidone (Resist remover 1165) at ≈70° C. for ≈15 min finished with a dump rinse. The next step is an acid clean with piranha solution (H_2SO_4:H_2O_2). The solution is used in a ratio of H_2SO_4:H_2O_2 (3:1) for ≈10 min, followed by a dump rinse. The last step is a solvent clean to remove the inorganic residuals of the ARC. The piranha solution can only remove the organic structure of the ARC but leaves the inorganic backbone of the resist on the surface. The recommended stripper for "AZ BARLi-II" is "AZ 300T stripper", which is used at ≈80° C. for ≈10 min, followed by a dry rinse and spin dry.

This lithography defines anchor holes, which go all the way down to the silicon handle wafer, to hold the released photonic structures in place. This requires a long etch process, which requires a UV cross linked resist to improve the resist performance during the etch. The first layer is an ARC which improves the adhesion between resist and sample. The ARC is followed by a layer of positive photo resist ("SPR 220-3"). A resist thickness of ≈3.1 μm has been chosen, because it supplies enough resist for the etch processes as well as good coverage of all topographical steps. The process parameters are as follows.

Resist layer 2: SPR-220 3

Spin speed: ≈10.5 rad/s (≈100 rpm) for ≈5 s/≈157 rad/s (≈1500 rpm) for ≈40 s

Soft bake: ≈115° C. for ≈90 s

The wafer is exposed with 200 mJ/cm^2, a focus of 1 μm, a numerical aperture of 0.48, and a sigma of 0.5 in the "conventional" illumination mode. The resist is treated with a post exposure bake, of ≈110° C. for ≈60 s, to improve the result of the lithography process. In the following, the structure is developed in "AZ 300 MIF" for ≈60 s followed by a DIW rinse and dried with nitrogen. Subsequently the wafer is exposed with UV light (≈300 kJ/cm^2) at a temperature of ≈90° C. This crosslinks the resist and lowers the etch rate in dry etch significantly.

The transfer process starts with a descum to remove the ARC at the bottom of the lithographically defined structures. The used oxygen plasma etch does only remove the organic part of the ARC the inorganic part will be removed in the following etch based on fluoroform (CHF_3) chemistry.

The etch step with fluoroform chemistry is used to etch through the LTO cladding layer, the silicon device layer, the buried oxide layer, and a few nm into the silicon handle wafer (FIG. **18***d*). The process parameters are summarized in table 10, the etch is performed in a parallel pate reactive ion etcher.

TABLE 10

Descum	
Tool:	RIE
Time:	≈7 min
Gases:	O_2/Ar
Flow rates:	≈5 ml/min (≈5 sccm)/≈20 ml/min (≈20 sccm)
Pressure:	≈4 Pa (≈30 mTorr)
RF power:	≈50 W
Ref. RF power:	≈0 W
SiO2	
Depth:	until the silicon handle wafer is reached
Gases:	O2/CHF3
Flow rates:	≈5 ml/min (≈5 sccm)/≈45 ml/min (≈45 sccm)
Pressure:	≈6.7 Pa (≈50 mTorr)
RF power:	≈200 W
Ref. RF power:	≈0 W
DC Bias:	≈516 V
Etch rate:	≈35 nm/min (SiO_2)/≈20 nm/min (Si)

The wafers are cleaned with a combination of solvents and acids to remove the plasma baked resist after the etching as well as the ARC. Followed by an RCA clean and a BOE etch to complete the thinning process as well as the formation of the anchor holes. The first step of the cleaning is using a solution based on N-Methyl-2-pyrrolidone (Resist remover 1165) at ≈70° C. for ≈15 min finished with a dump rinse. The next step is an acid clean with piranha solution (H_2SO_4:H_2O_2). The solution is used in a ratio of H_2SO_4:H_2O_2 (3:1) for ≈10 min, followed by a dump rinse. The last step is a solvent clean to remove the inorganic residuals of the ARC. The recommended stripper for "AZ BARLi-II" is "AZ 300T stripper", which is used at ≈80° C. for ≈10 min, followed by a dry rinse and spin dry. Subsequently an RCA clean as described earlier (3.1.5) is performed. The RCA clean is followed by a wet oxide etch to complete the thinning process as well as the formation of the anchor holes. Diluted buffered hydrofluoric acid (BOE 6:1) is used for this etch, because this acid smooths the oxide step but does not attack the interfaces between silicon and silicon dioxide, as would be attacked by diluted hydrofluoric acid. The sample is exposed to the diluted BOE (6:1) for ≈1 min and 30 s to remove ≈200 nm of silicon dioxide (FIG. **18***e*), followed by a dump rinse and dry.

Low stress silicon nitride is used as the mechanical material because it has high etch resistivity against hydrofluoric acid and potassium hydroxide. The final thickness of the silicon nitride layer is ≈400 nm with the net tensile stress of ≈300 MPa (FIG. **18***f*). The deposition is performed at ≈850° C. The wafer boat is filled with dummy wafers and one clean bare silicon wafer on both sides of the SOI wafer to aid in uniformity.

As relates to electrodes and wire bond pads, the metal lines and wire bond pads, to connect the cantilever chip to a printed circuit board (PCB), are created in a metal lift off process. The process is based on "Lift-off" resist in combination with a positive photoresist. Chromium and Gold (Cr/Au) are used as metals. The Cr functions as an adhesion layer for the Au. This combination is not attacked by the HF and KOH, and is stable to temperatures of up to 350° C. A stack of three resist layers is used for the "Lift-off" process. The first layer is the ARC, followed by a layer of "Lift-off" resist, and finalized by a layer of positive photo resist. "Lift-off" resist is usually based on the solvent 1-methoxy-2-propanol to avoid mixing with the positive photoresist, which is usually based on anisole as solvent. "Lift-off" resist is not photo sensitive and therefore it is non-selectively dissolved by the developer, which creates an undercut of the photoresist layer. This undercut can be tuned with the soft bake temperature and time and is very important for a clean and reproducible "lift-off" process. After the lithography process, the sample has to be treated with an descum process and a short etch based on fluoroform chemistry, to remove the ARC at the bottom of the lithographically defined structures, to expose the silicon nitride below. The short dry etch also etches into the silicon nitride which further improves the adhesion of the metal to the silicon nitride.

The resist stack starts with an ARC prepared as previously described. The second layer consist out of the "Lift-off"

resist ("LOR 3A") followed by a layer of positive photoresist. Parameters for the preparation of these three layers are listed in table 11.

TABLE 11

Resist layer 1: Barli II	
Spin speed:	≈10.5 rad/s (≈100 rpm) for ≈5 s/≈209.4 rad/s (≈2000 rpm) for ≈40 s
Soft bake:	≈200° C. for ≈60 s
Typ. thickness:	≈180 nm
Resist layer 2: LOR 3A	
Spin speed:	≈10.5 rad/s (≈100 rpm) for ≈5 s/≈314 rad/s (≈3000 rpm) for ≈40 s
Soft bake:	≈210° C. for ≈20 min
Typ. thickness:	≈300 nm
Resist layer 3: SPR-220 3	
Spin speed:	≈10.5 rad/s (≈100 rpm) for ≈5 s/≈314 rad/s (≈3000 rpm) for ≈40 s
Soft bake:	≈115° C. for ≈90 s
Typ. thickness:	≈1200 nm

The wafer is exposed with two different doses to clear the deep anchor hole and avoid overdosing the other structures. The first exposure is for all metal lines. This exposure uses 160 mJ/cm^2, a focus of 0.2 μm, a numerical aperture of 0.48, and a sigma of 0.5 in the "conventional" illumination mode. The second exposure is for all anchor holes and deep trenches. This exposure uses 200 mJ/cm^2, a focus of 0.6 μm, a numerical aperture of 0.48, and a sigma of 0.5 in the "conventional" illumination mode.

The resist is treated with a post exposure bake, of ≈110° C. for ≈60 s. In the following, the structure is developed in "AZ 300 MIF" for ≈60 s followed by a DIW rinse and nitrogen dry

As relates to descum and removal of the ARC, the transfer process starts with a descum to remove the ARC at the bottom of the lithographically defined structures. The etch step with fluoroform chemistry is used to remove the residual of the ARC and to etch into the first few nanometers of the silicon nitride layer for an improvement of the adhesion between the metal and the silicon nitride layer. The process parameters are listed in table 12, and the etch is performed in a parallel plate reactive ion etcher.

TABLE 12

Descum	
Tool:	RIE
Time:	≈7 min
Gases:	O_2/Ar
Flow rates:	≈5 ml/min (≈5 sccm)/≈20 ml/min (≈20 sccm)
Pressure:	≈4 Pa (≈30 mTorr)
RF power:	≈50 W
Ref. RF power:	≈0 W
ARC + SiN	
Time:	≈1 min
Gases:	O2/CHF3
Flow rates:	≈5 ml/min (≈5 sccm)/≈45 ml/min (≈45 sccm)
Pressure:	≈6.7 Pa (≈50 mTorr)
RF power:	≈200 W
Ref. RF power:	≈0 W
DC Bias:	≈516 V
Etch rate:	≈35 nm/min

The metal is deposited via evaporation. The adhesion of the metal layer is to the silicon nitride, wherein the descum is done shortly before the loading of the wafers. Furthermore, the Cr crucible is clean of any contamination. The Cr is deposited at a rate of 0.05 nm/s until a final thickness of 10 nm is reached. The Au is deposited at a rate of 0.25 nm/s until a final thickness of 120 nm is reached. "Lift-off" process is completed by dissolving the resist mask with a solvent solution based on N-Methyl-2-pyrrolidone at ≈70° C. for ≈3 h. The ARC is removed with piranha solution and "AZ 300T."

As relates to structuring of the mechanical member, the mechanical member of the transducer is shaped out of the silicon nitride layer. The shape is defined with a positive photoresist mask. Furthermore, the metal layer serves as a hard mask to improve the overlay error in critical regions. The lithography is based on ARC and positive photoresist. A dry etch process is used to transfer the structure into the silicon nitride layer. The etch chemistry based on fluoroform creates an etch rate of ≈60 nm/min for silicon nitride and ≈30 nm/min for the silicon dioxide layer underneath. The silicon nitride layer is over etched to ensure a good pattern transfer across all topographical steps.

The resist layers are prepared as described previously. The resist is exposed with 190 mJ/cm^2, a focus of 0.4 μm, a numerical aperture of 0.48, and a sigma of 0.5 in the "conventional" illumination mode. The resist is treated with a post exposure bake, of ≈110° C. for ≈60 s. In the following, the structure is developed in "AZ 300 MIF" for ≈60 s followed by a DIW rinse and nitrogen dry.

The pattern transfer starts with a descum step to remove the ARC at the bottom of the lithographically defined structures. The etch step with fluoroform chemistry is used to remove the residual of the ARC and to etch through the silicon nitride layer into the silicon dioxide layer. The process parameters are listed in table 13, and the etch is performed in a parallel pate reactive ion etcher.

TABLE 13

Descum	
Tool:	RIE
Time:	≈7 min
Gases:	O_2/Ar
Flow rates:	≈5 ml/min (≈5 sccm)/≈20 ml/min (≈20 sccm)
Pressure:	≈4 Pa (≈30 mTorr)
RF power:	≈50 W
Ref. RF power:	≈0 W
ARC + SiN + SiO_2	
Time:	≈1 min
Gases:	O2/CHF3
Flow rates:	≈5 ml/min (≈5 sccm)/≈45 ml/min (≈45 sccm)
Pressure:	≈6.7 Pa (≈50 mTorr)
RF power:	≈200 W
Ref. RF power:	≈0 W
DC Bias:	≈516 V
Etch rate:	≈60 nm/min (SiN)/≈30 nm/min (SiO_2)

The sample is cleaned with piranha solution followed by "AZ 300K."

As relates to hard mask preparation for anisotropic etch, in the following step, a hafnium oxide (HfO) hard mask is deposited on the wafer to protect the frontside, specifically the exposed areas of LTO, from potassium hydroxide (KOH), which is used to etch V-grooves into the frontside of the wafer and to shape the backside of the cantilever chip. The quality of the HfO layer is very important to ensure proper protection of the frontside. The etch rate of HfO in KOH depends on the carbon content of the HfO layer. The carbon content originates from the organic molecule (tetrakis(ethylmethylamino)hafnium (TEMAH)) which is used in the atomic layer deposition (ALD) process. The content of

carbon in the final layer can be lowered by the use of a plasma induced deposition and with an increase purge time, as well as purge flow rates. The HfO layer is later patterned with the openings for the KOH etch on the front- and backside of the wafer. The used process for the lithography and pattern transfer is very similar for both sides. The lithography is performed in a frontside and backside contact mask aligner lithography. The pattern is transferred with a sulfur hexafluoride chemistry into the HfO layer and a fluoroform chemistry for the transfer into the underlying $SiN/SiO_2/Si/SiO_2$ until the silicon handle wafer is reached.

As relates to hafnium oxide deposition, the parameters chosen for the HfO deposition are listed in table 14. The parameters are separated into the seven steps of the ALD process (surface cleaning, deposition, TEMAH dose, TEMAH purge, gas stabilization, O_2 plasma, plasma purge). The final thickness of the ALD layer is ≈20 nm, which provides enough protection against KOH and can encapsulate small contaminations on the wafer surface.

TABLE 14

Cleaning	
Recipe:	H2 surface clean
Pressure:	≈7.5 × 10^{-7} Pa
Gas:	H2
Flow rate:	≈15 ml/min (≈15 sccm)
Time (etch):	≈5 min
Temperature:	≈300° C.
Time (purge):	≈1 min
Deposition	
Recipe:	opt_HfO
Cycles:	200
Pressure:	≈7.5 × 10^{-7} Pa
Temperature:	≈300° C.
TEMAH dose	
Time:	≈0.6 s
Gases:	Ar/TEMAH
Flow rate:	≈250 ml/min (≈250 sccm)/≈1 mL/min (≈1 sccm)
TEMAH purge	
Time: ≈5 s	
Gases: Ar/O_2	
Flow rate: ≈100 ml/min (≈100 sccm)/≈50 mL/min (≈50 sccm)	
Opt_gas stabil	
Time: ≈1 s	
Gases: O_2	
Flow rate: ≈60 ml/min (≈60 sccm)	
O_2 plasma	
Time: ≈2 s	
Gases: O_2	
Flow rate: ≈60 ml/min (≈60 sccm)	

The wafer surface is prepared with hexamethyldiloxane. A thick positive photoresist is used to cover all topographical steps ("AZ 10xT"). The resist is applied with a spin coater with a spin speed of ≈10.47 rad/s (≈100 rpm) for ≈5 s followed by ≈418.88 rad/s (≈4000 rpm) for ≈45 s to create a final resist thickness of ≈10 μm. The resist is soft baked ≈110° C. for ≈180 s. The wafer is exposed in a mask aligner lithography with a dose of ≈1000 mJ/cm^2. The pattern is developed in diluted "AZ 400K" (1:3) for ≈180 s followed by a DIW rinse and dried with nitrogen

The pattern transfer starts with a sulfur hexafluoride chemistry to transfer the structure into the HfO layer. This etch is followed by an etch based on fluoroform chemistry to transfer the structure into the underlying $SiN/SiO_2/SiO_2/SiO_2$ until the silicon handle wafer is reached. The process parameters are listed in table 15, and the etch is performed in a parallel pate reactive ion etcher.

TABLE 15

HfO	
Tool:	RIE
Time:	≈5 min
Gases:	SF6/CF4
Flow rates:	≈6 ml/min (≈6 sccm)/≈24 mL/min (≈24 sccm)
Pressure:	≈1 Pa (≈8 mTorr)
RF power:	≈200 W
Ref. RF power:	≈0 W
DC Bias:	≈516 V
Etch rate:	≈10 nm/min (HfO)
$SiO_2/SiN/Si$	
Tool:	RIE Unaxis 790
Depth:	until the silicon handle wafer is exposed
Gases:	$O2/ChF_3$
Flow rates:	≈5 ml/min (≈5 sccm)/≈45 mL/min (≈45 sccm)
Pressure:	≈6.7 Pa (≈50 mTorr)
RF power:	≈200 W
Ref. RF power:	≈0 W
DC Bias:	≈516 V
Etch rate:	≈35 nm/min

As relates to backside lithography and pattern transfer, the process steps or previously described and or repeated on the backside of the wafer to define the openings for the backside anisotropic etching. The resist on the front side of the wafer is used as frontside protection during the backside lithography and pattern transfer process.

As relates to bulk micromachining, this step defines the frontside V-grooves for the fiber attachment and it shapes the cantilever chip to make it compatible with commercial scanning probe microscopes. The anisotropic etching process is separated into two parts. In the first part, the front- and backside are etched simultaneously until the V-grooves on the front side reach the final depth of ≈80 μm. At this point, the wafer is placed in an etch chuck to physically protect the frontside of the wafer from the etch solution and expose only the backside of the wafer. The backside is then etched until the backside etch reaches the frontside of the wafer and the membrane around the chip changes from a red, to an orange, and then to a clear color in the transmitted light. At this point, all the silicon on the membrane is gone and only the silicon dioxide membrane is left over.

The photoresist on the front- and backside of the wafer is removed with N-Methyl-2-pyrrolidone at ≈110° C. for ≈15 min followed by a dump rinse and spin dry.

The wafer is etched with a 30% solution of KOH in DIW at a temperature of ≈60° C. The beaker should be covered to avoid a change in concentration due to evaporation

Both sides are etched until the final depth of ≈80 μm for the frontside V-grooves is reached. At this point, the wafer is placed in an etch chuck to physically protect the frontside of the wafer from the etch solution and expose only the backside of the wafer. The etch is continued at ≈80° C. for ≈16 h. Until the backside etch reaches the front side of the wafer and the membrane around the chip changes from a red, to an orange, and then to a clear color in the transmitted light. At this point, all the silicon on the membrane is gone and only the silicon dioxide membrane is left over. Wafer can be removed from the chuck and cleaned in warm DIW several times followed by a clean in IPA and a careful drying with nitrogen.

As relates to release, the final release step consists out of a cleaning with HCl and DIW, followed by an HF sacrificial layer etch, which is completed with an intensive rinse with

DIW. After the DIW rinse, the wafer is placed into several batches of IPA to replace the DIW in all cavities with IPA. The wafer should stay in every bath for a couple of minutes. After all the DIW is replaced with IPA, the wafer is placed in a critical point dryer to critical point dry the released transducer.

As relates critical point drying, the release starts with a cleaning in HCl for ≈10 min to remove residuals of KOH followed by a dump rinse cycle until a sufficient bath resistivity is reached again. After the wafer is cleaned, the HfO protection layer and sio_2 sacrificial layer are etched in HF (49%) until all mechanical structures are sufficiently undercut. The release etch for the described structure is ≈4 min and 30 s, which results in an undercut of ≈7 μm. The HF etch is followed by extensive dump rinse cycles to remove all HF residuals form the substrate. In the following is the DIW replaced with IPA. This takes place in several bathes, each bath ≈10 min before the sample is placed in the critical point dryer to dry the released transducers.

While one or more embodiments have been shown and described, modifications and substitutions may be made thereto without departing from the spirit and scope of the invention. Accordingly, it is to be understood that the present invention has been described by way of illustrations and not limitation. Embodiments herein can be used independently or can be combined.

Reference throughout this specification to "one embodiment," "particular embodiment," "certain embodiment," "an embodiment," or the like means that a particular feature, structure, or characteristic described in connection with the embodiment is included in at least one embodiment. Thus, appearances of these phrases (e.g., "in one embodiment" or "in an embodiment") throughout this specification are not necessarily all referring to the same embodiment, but may. Furthermore, particular features, structures, or characteristics may be combined in any suitable manner, as would be apparent to one of ordinary skill in the art from this disclosure, in one or more embodiments.

All ranges disclosed herein are inclusive of the endpoints, and the endpoints are independently combinable with each other. The ranges are continuous and thus contain every value and subset thereof in the range. Unless otherwise stated or contextually inapplicable, all percentages, when expressing a quantity, are weight percentages. The suffix "(s)" as used herein is intended to include both the singular and the plural of the term that it modifies, thereby including at least one of that term (e.g., the colorant(s) includes at least one colorants). "Optional" or "optionally" means that the subsequently described event or circumstance can or cannot occur, and that the description includes instances where the event occurs and instances where it does not. As used herein, "combination" is inclusive of blends, mixtures, alloys, reaction products, and the like.

As used herein, "a combination thereof" refers to a combination comprising at least one of the named constituents, components, compounds, or elements, optionally together with one or more of the same class of constituents, components, compounds, or elements.

All references are incorporated herein by reference.

The use of the terms "a" and "an" and "the" and similar referents in the context of describing the invention (especially in the context of the following claims) are to be construed to cover both the singular and the plural, unless otherwise indicated herein or clearly contradicted by context. "Or" means "and/or." Further, the conjunction "or" is used to link objects of a list or alternatives and is not disjunctive; rather the elements can be used separately or can be combined together under appropriate circumstances. It should further be noted that the terms "first," "second," "primary," "secondary," and the like herein do not denote any order, quantity, or importance, but rather are used to distinguish one element from another. The modifier "about" used in connection with a quantity is inclusive of the stated value and has the meaning dictated by the context (e.g., it includes the degree of error associated with measurement of the particular quantity).

What is claimed is:

1. A photonic probe for atomic force microscopy comprising:

a substrate;

an arm disposed on the substrate and that extends beyond the substrate and that mechanically connects a cantilever and an optical resonator to the substrate;

the cantilever disposed on the arm and comprising:

a tip;

a wing in mechanical communication with the tip; and

an extension interposed between the tip and the wing to synchronously communicate motion of the tip with the wing;

an anchor interposed between the arm and the cantilever and that attaches the cantilever to the arm;

the optical resonator disposed proximate to the cantilever and that:

receives input light; and

produces output light,

such that:

the cantilever is spaced by a gap distance from the optical resonator,

wherein the gap distance varies as the cantilever moves relative to the optical resonator, and

the output light differs from the input light in response to movement of the cantilever relative to the optical resonator;

a connector interposed between the arm and the optical resonator and that attaches the optical resonator to the arm such that the optical resonator is suspended from a cover layer via the arm and the connector;

an optical waveguide disposed on the substrate and in optical communication with the optical resonator and that:

provides the input light to the optical resonator; and

receives the output light from the optical resonator; and

the cover layer disposed on the substrate such that a portion of the arm and the optical waveguide are interposed between the cover layer and the substrate, and the optical resonator and the cantilever do not overlap with the cover layer so that the optical resonator and the cantilever are exposed and not covered by the cover layer and the substrate,

wherein the cantilever and the optical resonator protrude from the substrate and do not spatially overlap the substrate, and the cantilever flexes independently of the substrate.

2. The photonic probe of claim **1**, further comprising:

an optical cladding layer interposed between the cover layer and the substrate.

3. The photonic probe of claim **2**, wherein the cantilever mechanically deforms in response to mechanical contact between the tip and an object disposed proximate to the tip.

4. The photonic probe of claim **1**, wherein the optical resonator comprises a photonic crystal.

5. The photonic probe of claim **4**, wherein the optical waveguide is in mechanical communication with the photonic crystal.

6. The photonic probe of claim 1, wherein the input light comprises a wavelength from 400 nm to 2 μm.

7. The photonic probe of claim 1, wherein the output light comprises a wavelength from 400 nm to 2 μm.

8. The photonic probe of claim 1, wherein the gap distance is from 50 nm to 1 μm.

* * * * *